Post-Glacial Inflation-Deflation Cycles, Tilting, and Faulting in the Yellowstone Caldera Based on Yellowstone Lake Shorelines

By Kenneth L. Pierce[1], Kenneth P. Cannon[2], Grant A. Meyer[3], Matthew J. Trebesch[1], *and* Raymond D. Watts[4]

Open-File Report 02-0142

2002

U.S. DEPARTMENT OF THE INTERIOR
U.S. GEOLOGICAL SURVEY

[1] Bozeman, Montana
[2] National Park Service
[3] University of New Mexico
[4] Fort Collins, Colorado

Post-Glacial Inflation-Deflation Cycles, tilting, and faulting in the Yellowstone Caldera Based on Yellowstone Lake Shorelines

Kenneth L. Pierce, U.S. Geological Survey, Northern Rocky Mountain Science Center (NRMSC), Box 173492, Montana State University, Bozeman, MT 59717, kpierce@usgs.gov;
Kenneth P. Cannon, National Park Service, Midwest Archeological Center, Federal Building, Lincoln, NE 68508-3873, ken_cannon@nps.gov;
Grant A. Meyer, Department of Earth and Planetary Sciences, University of New Mexico, Albuquerque NM 87131-1116, gmeyer@unm.edu
Matthew J. Trebesch, U.S. Geological Survey, NRMSC, Bozeman, MT
Raymond Watts, U.S. Geological Survey, 4512 McMurry Av., Fort Collins, CO 80525-3400, rwatts@usgs.gov

1. Abstract

The Yellowstone caldera, like many other later Quaternary calderas of the world, exhibits dramatic unrest. Between 1923 and 1985, the center of the Yellowstone caldera rose nearly one meter along an axis between its two resurgent domes (Pelton and Smith, 1979, Dzurisin and Yamashita, 1987). From 1985 until 1995-6, it subsided at about two cm/yr (Dzurisin and others, 1990). More recent radar interferometry studies show renewed inflation of the northeastern resurgent dome between 1995 and 1996; this inflation migrated to the southwestern resurgent dome from 1996 to 1997 (Wicks and others, 1998).

We extend this record back in time using dated geomorphic evidence of postglacial Yellowstone Lake shorelines around the northern shore, and Yellowstone River levels in the outlet area. We date these shorelines using carbon isotopic and archeological methods. Following Meyer and Locke (1986) and Locke and Meyer (1994), we identify the modern shoreline as *S1* (1.9 ± 0.3 m above the lake gage datum), map paleoshoreline terraces *S2* to *S6*, and infer that the prominent shorelines were cut during intracaldera uplift episodes that produced rising water levels. Doming along the caldera axis reduces the gradient of the Yellowstone River from Le Hardys Rapids to the Yellowstone Lake outlet and ultimately causes an increase in lake level. The 1923-1985 doming is part of a longer uplift episode that has reduced the Yellowstone River gradient to a "pool" with a drop of only 0.25 m over most of this 5 km reach. We also present new evidence that doming has caused submergence of some Holocene lake and river levels.

Shoreline *S5* is about 14 m above datum and estimated to be ~12.6 ka, because it post-dates a large hydrothermal explosion deposit from the Mary Bay area (MB-II) that occurred ~13 ka. *S4* formed about 8 m above datum ~10.7 ka as dated by archeology and ^{14}C, and was accompanied by offset on the Fishing Bridge fault. About 9.7 ka, the Yellowstone River eroded the "S-meander", followed by a ~5 m rise in lake level to *S2*. The lowest generally recognizable shoreline is *S2*. It is ~5 m above datum (3 m above *S1)* and is ~8 ka, as dated on both sides of the outlet. Yellowstone Lake and the river near Fishing Bridge were 5-6 m below their present level about 3-4 ka, as indicated by ^{14}C ages from submerged beach deposits, drowned valleys, and submerged Yellowstone River gravels. Thus, the lake in the outlet region has been below or near its present level for about half the time since a 1 km-thick icecap melted from the Yellowstone Lake basin about 16 ka.

The amplitude of two rises in lake and river level can be estimated based on the altitude of Le Hardys Rapids, indicators of former lake and river levels, and reconstruction of the river gradient from

the outlet to Le Hardys Rapids. Both between ~9.5 ka and ~8.5 ka, and after ~3 ka, Le Hardys Rapids (LHR) was uplifted about 8 meters above the outlet, suggesting a cyclic deformation process. Older possible rises in lake level are suggested by locations where the ~10.7 ka *S4* truncates older shorelines, and valleys truncated by the ~12.6 ka *S5* shoreline. Using these controls, a plot of lake level through time shows 5-7 millennial-scale oscillations since 14.5 ka.

Major cycles of inflation and deflation are thousands of years long. Le Hardys Rapids has twice been uplifted ~8 m relative to the lake outlet. These two locations span only the central 25% of the historic caldera doming, so that if we use historic doming as a model, total projected uplift would be ~32 m. This "heavy breathing" of the central part of the Yellowstone caldera may reflect a combination of several possible processes: magmatic inflation, tectonic stretching and deflation, and hydrothermal fluid sealing and inflation followed by cracking of the seal, pressure release, and deflation. Over the entire postglacial period, subsidence has balanced or slightly exceeded uplift as shown by older shorelines that *descend* towards the caldera axis. We favor a hydrothermal mechanism for inflation and deflation because it provides for both inflation and deflation with little overall change. Other mechanisms such as inflation by magma intrusion and deflation by extensional stretching require two separate processes to alternate and yet result in no net elevation change.

In addition to inflation and deflation, new LIDAR data demonstrates previously unrecognized local deformation along the north shore of Yellowstone Lake. The newly recognized Fishing Bridge fault shows a progressive increase in offset from 0.5 m for the ~8 ka *S2* to perhaps 5 m for the ~12.6 ka *S5*. Uplift of the Storm Point hydrothermal center tilts shorelines westward as much as 6 m over one kilometer. A local anticline has as much as 3 m relief in 0.5 km. LIDAR data also shows the Mary Bay II hydrothermal explosion debris has a surface relief of about 1 m over 100 m, and that it overlies S5.5 and *S6* shorelines, but not *S.*

Although the postglacial deformation record does not indicate voluminous magma accumulation or other large-scale eruption precursors, strong local deformation associated with hydrothermal centers does suggest the possibility of future hydrothermal explosions and associated hazards.

Introduction

The Yellowstone caldera is the youngest of three large rhyolitic calderas formed in greater Yellowstone in the last 2.1 Ma (Christiansen, 1984, 2001). It collapsed with eruption of ~1000 km^3 of ash flows from two overlapping ring-fracture systems at ~630 ka. The two collapse centers were uplifted shortly thereafter into the Sour Creek (northeast) and Mallard Lake (southwest) resurgent domes. Voluminous extrusion of rhyolitic lavas from 150 ka to 70 ka covered much of the caldera excepting the Sour Creek dome, Pelican Valley and much of the eastern part of Yellowstone Lake. At present, this caldera shows remarkable signs of unrest, consistent with many other young calderas around the world (Newhall and Dzurisin, 1988; Dvorak and Mastrolorenzo, 1991). A resurvey of 1923 level lines in 1975-1977 along the road system of Yellowstone showed doming within the caldera (Fig. 1), with maximum uplift at Le Hardys Rapids (LHR) of about 0.8 m (Pelton and Smith, 1979). Between 1976 and 1985, resurveys revealed an additional 0.15 m uplift of LHR, with a pattern similar to that between 1976 and 1986 (Dzurisin and Yamashita, 1987). Thus, from 1926 to 1985, maximum uplift was about 0.95 m over

62 years at an average rate of about 15 mm/yr. Uplift unexpectedly ceased in 1985, and between 1986 and 1996, the caldera subsided at a maximum rate of about 20 mm/yr in a pattern essentially inverse to the uplift (Fig. 3). Recent radar interferometry studies define a more complex temporal pattern, with renewed inflation of the Sour Creek resurgent dome area from 1995 to 1996, and migration of inflation to the Mallard Lake dome area from 1996 to 1997 (Wicks and others, 1998). GPS measurements from 1987 to 1995 (Smith and others, 1997; Meertens and others, 2000) show caldera-wide subsidence up to 15 mm/yr accompanied by radial-caldera contraction at 15 mm/yr**.**

Spurred by these records of uplift and subsidence in the Yellowstone caldera over the last century, we employed geomorphic criteria to assess the character and magnitude of deformation over the last 15,000 years. Paleoshorelines of Yellowstone Lake and drowned subaerial features such as stream valleys and beach sediment allow us to construct a record of vertical deformation in the central part of the Yellowstone caldera. New ^{14}C and projectile-point ages obtained in archeological surveys and excavations as well as geological studies provide improved age control (Pierce and others, 1994; Cannon and others, 1994, 1995, 1996). Cyclic inflation and deflation of the caldera in the last 100 years has been called "breathing" (e.g., Pelton and Smith, 1979); we use the term "heavy breathing" for longer, higher amplitude cycles of inflation and deflation.

We build this study on the detailed surveying of Yellowstone Lake shorelines by Meyer and Locke (1986), Locke (1986), Meyer (1986), and Locke and Meyer (1994). Our findings are in general agreement with their mapping and correlation of shorelines; however, new dating and archeological studies indicate that the lower shorelines are much older than previously thought. LIDAR imagery of the northern lakeshore permits more continuous tracing and elevation measurement of shorelines, and revision of some shoreline correlations east of Pelican Creek. LIDAR imagery also allowed us to locate previously unrecognized features, including the Fishing Bridge fault and low-relief beach-ridge shorelines that are strongly tilted away from the Storm Point geothermal center.

2A. Previous studies of post-glacial shorelines. Richmond first mapped shorelines from 3 to more than 50 m above present Yellowstone Lake (Richmond, 1973, 1974, 1976; 1977; Richmond and Pierce, 1972). He considered shorelines at and below 18-20 m to represent an open, post-glacial lake, whereas higher shorelines were associated with deglaciation of the lake basin. Richmond's work pre-dated recognition of active deformation in the Yellowstone caldera, and he assumed (1) that shorelines could be correlated by height alone, and (2) that lake level underwent a relatively simple and continuous decline over postglacial time.

Drawing on this earlier work, Meyer and Locke (1986) mapped and correlated about nine shorelines around northern Yellowstone Lake. They designated the present shoreline as *S1,* and shorelines up to about 30 m above present as *S2* to *S9*. Shoreline profiles were surveyed to centimeter accuracy (with closure) using the Bridge Bay lake gage zero mark as a datum, and shoreline elevations interpreted to the decimeter. Meyer and Locke (1986) inferred that prominent shorelines were cut by rising lake levels due to episodic uplift within the Yellowstone caldera. This work was later continued around the entire lake (Locke and Meyer, 1994). In contrast to earlier work, which relied on rapid hand leveling, these studies showed that many shorelines were deformed, both inside and outside of the caldera. Except for local

areas of greater tilting and faulting, however, most shorelines were found to be gently warped. Given that historic intracaldera uplift and subsidence rates of 10-20 mm/yr could produce 50-100 m vertical deformation in 5,000 yr, Locke and Meyer (1994) noted that net intracaldera deformation over the Holocene must be small, since most shorelines are sub-horizontal and the highest, oldest postglacial shorelines are at similar elevations inside and outside of the caldera (± ~8 m). In these studies, a small number of radiocarbon dates were obtained on organic matter in lagoonal sediments associated with shorelines, but these provided only minimum ages.

During archeological studies near the outlet of Yellowstone Lake, Reeve (1989) initially recognized a discrepancy between Richmond's declining lake model and the occurrence of Late Pleistocene-early Holocene (Paleo-Indian) projectile points within a few meters of present lake level, but he did not note that his archeological studies required considerably older ages than the minimum-limiting dates of Meyer and Locke (1986). Hamilton and Bailey (1990) recognized submerged shorelines of Yellowstone Lake at depths of 3-30 m below the present lake surface and constructed a complex history of post-glacial lake level changes, but with little age control or means of correlation. Submerged shorelines are also described by Johnson and others (submitted).

3. Holocene lake and river level changes and their chronology

In this section we present the data used to construct the detailed lake-level chronology of Figure 4. Table 1 describes the radiocarbon ages, and gives the calibrated (calendar) ages. Elevation is relative to the Bridge Bay gage. We first present evidence for low lake and river levels that were followed by a *rise* in lake and river levels, because this is the key observation indicating caldera inflation. We then describe subaerial shorelines in order of *increasing* age because this is how we resolved the chronology shown in Figure 4.

Airborne LIDAR (Light Detection and Ranging) elevation data were incorporated into this study. The survey contractor, Eaglescan, Inc., flew its instrumented airplane approximately 1,500 m above ground level. Aircraft position was recorded using base-station-corrected global positioning system (GPS) measurements, and aircraft attitude was measured with an inertial navigation system (INS). The laser was in the near infrared wavelength (1.069 microns) and recorded returns from the land and water surface, reflecting these from a cross-track scanning mirror. The same laser that generated the transmissions amplified ground-return pulses for detection and measurement of the round-trip time of light. Recording equipment was configured to log the last return pulse, thus discarding a large fraction of vegetation signals. Each lidar pulse was approximately 15 cm thick along its flight path (this is the instrumental resolution limit for elevation determinations), and approximately 1 m in diameter at its intersection with the ground.

The contractor's post-flight data processing combined GPS positions, INS attitude measurements, mirror positions, and laser-pulse time-of-flight measurements to determine the georeferenced location of each reflection point in UTM coordinates (Zone 12, WGS84 reference system). The scanning mirror operated within 15 degrees of nadir, measuring a swath width of 800 m along each flight line. Geometric factors degrade the accuracy of position determinations at points farther from nadir; errors at 15 degrees

are approximately 1 m. The laser pulse repetition frequency and mirror scan rate were sufficient to sample elevations at a nominal 2 m spacing across-track and 5 m spacing along track.

Post-flight processing included winnowing of returns that came from vegetation and other features above the mean neighborhood surface. The remaining returns, presumed to come from the ground or from low ground-cover vegetation, defined a triangulated irregular network (TIN). The data were interpolated to a 2-meter square grid by sampling the triangular facets of the TIN at the grid points. We used the lake level gage at Bridge Bay Marina, 1.45 ft (0.44 m) when the LIDAR was flown, to calibrate to the datum used in previous studies (e.g., Meyer and Locke, 1986). The altitude of the zero mark on the gage was measured at 2356.48 m in 1985 by level surveys.

3A. Lake level rises after lake lows 3-4 ka, and 9.5 ka

3A1. Yellowstone Lake.

Many of the lower ends of stream valleys entering Yellowstone Lake appear to be drowned. Several streams both north and south of the West Thumb Geyser Basin have drowned valleys upstream from their entrances into Yellowstone Lake, commonly with standing water grading upstream into alluvial wetlands. Two such streams are Thumb Creek and Little Thumb Creek (Fig. 2). The next stream north of Little Thumb Creek (here called "Little Thumb Creek North") has water standing in a drowned valley on the upstream (west) side of the highway. Highway borings in the center of this drowned valley encountered wood at a depth of –4.3 m below datum with an age ~3.0 ka (2,880 ± 60 yr BP; Table 1, #6). Insect faunae studied by Scott Elias (written commun., 1993) indicate a shallow wetland environment was associated with the wood. Since this time, the level of Yellowstone Lake has risen about 5-6 m, but this small stream has not yet transported enough sediment to fill in the drowned valley.

Immediately offshore from the West Thumb Geyser Basin, aprons of siliceous sinter around active and inactive hydrothermal vents extend well below lake level. Divers from the National Park Service sampled these vents at depths of 16 and 18 feet (4.9 and 5.5 m) below datum. Analysis of the oxygen isotope composition show it formed subaerially, and not under Yellowstone Lake (Pat Shanks, oral commun., 2000). Shoreline data (Locke, 1986; Locke and Meyer, 1994) also suggest substantial local downwarping in the West Thumb area, although the lower shorelines are poorly defined and correlated there.

We cored Yellowstone Lake about 6 km southwest of the outlet in the relatively quiet water of Bridge Bay, which is sheltered from wave action generated by the prevailing southwesterly winds. A wood sample from a coarse sand deposit 5 m below the surface (3.45 m below datum) yielded an age of ~3.8 ka (3,560 ± 60 yr BP, Table 1, #7). The sand is well-sorted and 0.5 m thick, similar to the modern beach. It is underlain by firm deep-water lake sediments, and overlain by poorly consolidated, fine deep-water sediments. We infer that the sand represents a beach deposit drowned by a lake-level rise after ~3.8 ka). This site is 3.2 km west of the north-trending Lake Hotel fault and thus its submergence is not related to downdropping on that fault.

Two other drowned valleys adjacent to Yellowstone Lake and cored by Federal Highways Administration indicate low lake levels. (1) Pelican Creek is a drowned valley as suggested by the high,

steep stream-cut scarps that now flank the exceptionally wide, low-gradient floodplain. An aggrading stream will have a wide valley and the necessity of the aggrading stream at times occupying the valley edge where it can undercut the banks are part of this process. Borings for a proposed causeway across Pelican Creek encountered gravelly sands above finer lake sediments. These gravelly sands extend to a depth of 4 to 5 m below datum. We interpret the gravelly sand to represent a drowned channel of Pelican Creek eroded into lake sediments. Although no carbon samples were obtained from the gravelly sand, an age of ~13.8 ka (11, 720 ± 60 yr BP, Table 1) was obtained from the lake sediments just below the gravelly sands. (2) Sedge Creek is nearly at the caldera margin and has a similar lower valley to Pelican Creek. At Sedge Creek, gravelly sediment extends to 18 m below datum and is underlain by about 6 m of fine-grained lake sediment that overlies a lower gravelly material, possibly glacial till or outwash. This suggests the possibility of a drowned valley extending to 18 m below datum only 0.5 km from the caldera boundary near Lake Butte.

3A2. Outlet Reach of the Yellowstone River

The outlet reach of the Yellowstone River (Fig. 5) is anomalous and extends from the outlet at Fishing Bridge to Le Hardys Rapids (LHR). The river has recently deposited sandbars in the *outsides* of meanders, effectively straightening its channel and indicating a substantial reduction in stream power (Meyer, 1986, Fig 17; Locke and Meyer, 1994). The present river has very low gradient (0.05 m/km). For low discharge in September, both surveying (Dan Dzurisin, spoken commun., 1993) and LIDAR data indicate a total drop of only 0.25 m in the 5 km from the outlet to just upstream from LHR. During higher discharges in June, the water surface would have a somewhat steeper gradient. The only bedrock forming the channel bed in this reach is at LHR, where an erosionally resistant unit in the Lava Creek Tuff acts as a weir that controls water level in the outlet reach (Hamilton, 1987). Uplift or subsidence of this bedrock threshold therefore has the potential to control both the river gradient and the level of Yellowstone Lake. Downstream from LHR, the river has a gradient of 1.8 m/km, more than 30 times steeper than above LHR.

Although the river is now essentially a continuous, low-velocity "pool" in the outlet reach, steep, high cutbanks on the outsides of the meanders indicate that the older, more sinuous channel contained an energetic river (Fig. 5). These scarps were so actively being undercut that they were unvegetated and served as a source for thick eolian sand now preserved at the top of the bank (Figs. 5, 8). About 1 km downstream from the outlet, an outer meander of the old channel forms a slough that is isolated from the present active channel by a sand bar.

A core in this slough encountered 3.5 m of fine sediment over river gravel at 4 m (3.4 m below datum). The gravel is at least 1 m thick; wood and charcoal samples from the upper gravel yielded ages of ~2.8 ka (2,710 ± 60 and 2,750 ± 86 yr BP, Table 1, # 4, 5). We infer that the gravel represents a reduction of gradient and velocity because of relative uplift of the bedrock threshold at LHR downstream, and that the fine sediment has accumulated since abandonment and drowning of the channel bend. The top of the river gravel is now about 3 m *below* the threshold at LHR, whereas at the time of deposition it would have been significantly above the threshold.

Therefore, at the time of active transport of the river gravels, the Yellowstone River had a considerably steeper gradient and sufficient energy to undercut banks 15 m high. Based on median sediment diameter of 1.5 cm and 1.5 m water depth, Waite Osterkamp (written commun., 1996) used the Shields equation to estimate the paleo-river gradient of 1m/km for significant transport of 1.5 cm gravel and 0.5 m/km for incipient transport. Figure 6 shows a graphical solution for the uplift of LHR relative to the core site. With a gradient of 1m/km, uplift is 7.5 m, and if this gradient is extended from the core site to the outlet, is 8.5 m. We acknowledge this paleo-river gradient is poorly constrained and only estimated at one site. Consideration of potential errors indicates that the gradient could have been as low as 0.5 m/km, therefore a drop of 2.5 m over the 5 km outlet reach. This yields a minimum estimated uplift of LHR of 5.5 m relative to the outlet (Fig. 6).

3B. S-meander and rise of lake ~9.7-8.6 ka

The "S-meander" is an abandoned (relict) set of meander bends of the Yellowstone River about 1-2 km north of the outlet (Fig. 5). The downstream meander bend was partly filled with a sand bar or spit during a rise of Yellowstone Lake (Meyer and Locke, 1986, Locke and Meyer, 1994). LIDAR data and field measurements show this sand spit is offset 1.2-1.8 m by the Fishing Bridge fault (Fig. 8). Data from the S-meander indicate that the former vigorous river at ~ 9.7 ka was converted to an arm of Yellowstone Lake by ~ 8.6 ka (Fig. 4).

A trench in the S-meander on the east side of the river revealed buried charcoal resting on channel gravels, showing that drowning of the river was underway by 9 ka (8,200 yr BP; Fig. 7, Table 1, # 17. 18, 19). The full suite of landforms and dated river and shoreline deposits on both sides of the modern Yellowstone River imply the following sequence: (1) formation of the S-meander with river transport of 3 cm gravel and vigorous bank undercutting to produce steep scarps 15 m high; (2) loss of current and cessation of gravel transport and deposition of charcoal by 9 ka; (3) continued drowning until Yellowstone Lake rose into this area and cut the *S3* shoreline into the meander scarp at 5.5 m above datum, perhaps ~8.6 ka; (4) lowering of the lake about 2 m and cutting of the *S2* shoreline at ~4.1 m above datum, dated nearby to ~ 8.1 ka, and (5) lowering of lake and river to levels below present by 3-4 ka (Fig. 4).

The drowning of the S-meander is a remarkably similar event to the more recent drowning of the Yellowstone River, particularly the increase in water level to 4-5 m above channel gravels (compare Figs. 6, 7, 8, 9). We postulate that uplift centered on LHR is also responsible for drowning of the S-meander. A field estimate of the median gravel diameter in the S-meander is ~3 cm, twice that noted in the present drowned channel that was active about 3 ka. A median diameter of 3 cm with a 1.5 m water depth yields a gradient of 1 m/km for incipient movement of pebbles and 2 m/km for significant transport of pebbles. We use the conservative 1m/km gradient in Figure 9, because some coarser gravel may have been introduced into the stream channel from the high, adjacent cutbank in sandy gravel ("plsg", Pinedale lacustrine sandy gravel; Richmond, 1977). This 1m/km gradient yields uplift of LHR relative to the trench site of 7.3 m and 8.3 m relative to the outlet (Fig. 9). If we use the 2-m/km gradient, then uplift of LHR relative to this S-meander site would be 11.3 m, and 13.3 m relative to the lake outlet. The S-meander is drowned at its downstream end by the present river, which may reflect a combination of uplift

downstream by either warping or faulting, and drowning associated with post-3 ka uplift discussed earlier.

3C. Sub-aerial shoreline sequence, ~8.0 ka S2 to ~14.4 ka S6

***S2* shoreline**-. Numerous ages on both sides of the outlet date the *S2* shoreline as about 8.0 ka (Fig. 4). Directly in front of the Lake Lodge, lagoonal sediments between the wave-cut *S2* shoreline and its barrier beach (now partly eroded) are exposed in the present wave-cut bluff. Two charcoal samples from the upper part of these diatomaceous sediments above cross-bedded sands yielded ages of 8.0 ka (7,210 ± 60 and 7,210 ± 50 yr B.P., Table 1, #14, 15; Fig. 4). Other samples from or above a humic soil that is below *S2* and clearly post-dates it yield ages of 6.0, 5.3-5.5, 4.7-4.8, and 4.6-4.8 ka (~5,300, 4,710, 4,160, and 4,110 yr BP, Table 1, #10, 9, 8, & not numbered) and thus provide additional support for the surprisingly old age of ~8.0 ka for *S2*.

On the Fishing Bridge peninsula East of the outlet, a sample from beneath a 2 m thick eolian sand mantling *S2* yielded an age of 7.6-7.7 ka (6,800 ± 90 yr BP, Cannon and others, 1994, Fig. 40). Just east of this site, a terrace of Pelican Creek truncates *S2*. A sample from a paleochannel on this terrace yielded an age of 7.6 ka (6,740 ± 90, Table 1). We infer an age for *S2* of ≥~8 ka or 0.4 ka older than this minimum age in that following deposition of *S2*, (1) lake level lowered and a wide terrace of Pelican Creek formed and eroded out *S2*, and (2) that an active channel on this terrace was abandoned and then accumulated charcoal bearing sediment about 7.6 ka. A mid-Holocene projectile point was collected from the surface of the *S2* in the old campground loops D and E (Cannon and others 1997: Fig. 41h). The eared and basally notched point is similar to those recovered from Layer 30 at Mummy Cave dated ~5 ka (4,420 ± 150 yr BP, Husted and Edgar, 2001).

Southeast of Yellowstone Lake and 4 km upstream from the margin of the Yellowstone River delta is a terrace of an older delta with a prominent paleo-distributary channel graded to ~7-8 m above datum (Fig. 2). Local damming of this channel has facilitated accumulation of more than 2 m of organic-rich sediment. Wood from a depth of 2.15 m just above channel sands in this paleochannel is 7.8 ka (6,990 ± 40 yr BP, Table 1, part I). Trail Lake (Fig. 2) is also dammed by this paleodelta. Basal ages from Trail Lake are 8.0 ka (7,215 ± 70 yr BP, Cathy Whitlock, spoken commun., 1999). These ages of 7.8 to 8.0 ka are essentially the same as those for the *S2* shoreline in the outlet area. Thus, a delta at ~7-8 m above datum well outside the Yellowstone caldera has similar ages to the *S2* shoreline 4-5 m above datum in the outlet area. This difference of 2-4 m over a distance of 34 km yields an overall tilt of only 0.06- 0.1 m/km towards the caldera center.

***S3* shoreline**-. The *S3* shoreline is mapped in the area from the Lake Lodge to the outlet and east of Pelican Creek, but is not well represented on the Fishing Bridge peninsula (Meyer and Locke, 1986). *S2* and *S3* are best represented in the S-meander by the tops of two small deltas that were built into the S-meander by the drainage that comes from the sewage disposal plant area at 5.5 (*S3*) and 4.75 m (*S2*) above datum (Fig. 5). *S3* does not appear to be readily recognizable and seems closely linked with *S2,*

and is here locally referenced as *S2/S3*. Gravelly deposits at the approximate altitude of *S3* do occur in the paleolagoon of the *S4* shoreline on the Fishing Bridge peninsula. There, at an elevation of 4.75 m above datum and at a depth of one meter and just above well-sorted sands is charcoal with an age of 8.2-8.5 ka (7,565 ± 70 yr BP, Cannon and others, 1994, Fig. 14). Excavations by SUNY-Albany also produced two large side-notched projectile points from the inferred position of the *S3* shoreline in the *S4* Fishing Bridge paleolagoon (Reeve 1989:Figure 13h and 13i). One point is similar to the Blackwater side-notched projectile point style recovered from Layer 16 in Mummy Cave and radiocarbon dated 8.0-9.0 ka (7,630 ± 170 yrs BP, Husted and Edgar 2001). The depth of the *S4* paleolagoon is such that in *S3*, and perhaps *S2* time, Yellowstone Lake may have extended into the northern part of this lagoon.

***S4* shoreline**-. On the Fishing Bridge peninsula, a wave-cut shoreline and a barrier beach to the south, with an intervening paleolagoon, represent the S4 shoreline. The Hamilton Store at Fishing Bridge lies on the crest of the *S4* barrier beach. In the old Fishing Bridge campground area, archeological excavations commonly exposed a meter or more of eolian sand overlying *S4* barrier-beach gravels. Charcoal ~10.2 ka (8940 ± 60 yr BP) was collected from 1.6 m depth in disturbed sediment filling the root void of a tree throw in beach gravel. The beach gravel is covered with 1.3 m of mixed material mostly of eolian sand (Cannon and others, 1994, Fig. 44).

Two Scottsbluff projectile points and one Cody Knife from the late Paleoindian Cody Cultural Complex have been found on the *S4* barrier beach (Figure 11). Ages for the Cody Cultural Complex range from 9.7-10.6 ka (8,800 to 9,400 yr BP, Frison 1991:66, Table 2.2) and support an age of ~ 10.7 ka for *S4*. Six additional late Paleoindian projectile points were recovered from excavations on the S4 surface on the Fishing Bridge peninsula. These stylistically variable projectile points conform to lanceolate projectile point styles of the Foothills-Mountains tradition that date between 8.8? and 10? ka (8,000 and 9,000 yr BP; Frison, 1992).

On the south shore of West Thumb, similar constraints for the age of *S4* are found at the Osprey Beach archeological Site (48YE409) 3 km east of Grant Village (Fig. 2). A gravel bench at 6.4 m above datum extends back to a nearby wave-cut shoreline ~6.8 m above datum. Bill Locke (written commun., 2001, profile Z54) places *S4* at 7.0 and *S5* at 8.8 m above datum nearby. Just above beach gravels and beneath 60 cm of non-bedded mixed material (pebbly sand of largely eolian origin), charcoal is 10.3-10.7 ka (Table 1). Cody Complex material was found in the basal part of the mixed zone just above the beach gravels, as well as recently slumped from the wave-cut cliff onto the modern beach below (Shortt, 2001). Cody Complex ages are from 9.7-10.6 ka (see discussion above for age). A Goshen (or Plainview?) point was also found 30 m back from the bluff (Don Blakeslee, written commun., map, 2002). Goshen (or Plainview) points are perhaps 500 years older than the Cody Complex, or ~10 to 11.6 ka (Ann Johnson, personal commun., 2002). This may indicate a slightly older age for this shoreline than *S4* in the Fishing Bridge area, although because occupation of the shoreline follows its formation, the ages also may be the same.

***S5* Shoreline-.** We trace S5 along the north shore of Yellowstone Lake and along the present outlet reach of the Yellowstone River. LIDAR imagery (Fig. 10) shows that *S5* on the east side of Pelican

Creek probably extends east to the shoreline that Meyer and Locke (1986) mapped as *S6* near Mary Bay. The LIDAR imagery also shows a deposit with hummocky surface texture above and north of *S5* with a relief of about 1 m over 50-100 m (Fig. 13). We identify this as the last large hydrothermal explosion deposit from Mary Bay exposed on land and designate it as Mary Bay II (MB II). In the bluffs south of Indian Pond, MB II overlies sandy lake sediment that contains charcoal at 2.6 m below MB II that dates 11.3-13.4 ka (10,720 ± 350, Richmond, 1977). The sandy lake sediment grades downward into coarsely varved lake sediment that contains ash 4.6 m below the MB II. The ash contains a mixture of shards probably from the Glacier Peak ash (layers B or G) apparently contaminated by reworked shards from a Yellowstone source (Andre Sarna-Wojcicki, written commun., 1999). Several dated localities place the age of Glacier Peak ash at between ~13.4 and 14 ka (Table 1). In the Yellowstone-Grand Teton region, Whitlock (1993) obtained ages of 13.4-14.1 ka for a Glacier Peak ash (Table 1, 11,450 and 12,100 yr BP). Although a Glacier Peak ash in west central Montana has been dated as 13.2 ka Table 1, 11,200 yr BP; Mehringer and others, 1984), studies in west central Idaho indicate an age older than 13.4 ka (Table 1, 11,510 ± 70 yr BP; Doerner and Carrara, 2001). Based on the charcoal and ash ages and assuming that the lake sediment accumulated rapidly, we estimate an age of ~13 ka for the MB-II hydrothermal explosion deposits and ~12.6 ka for the *S5* shoreline (Fig. 4). The *S5* shoreline is the highest shoreline eroded into the steep crater walls on the northern part of Mary Bay, which also shows that *S5* formed soon, after the MB II explosion, for S5.5 is not found higher on the crater wall. The *S5* shoreline is now tilted down towards the caldera axis (Fig. 12). From 16-17 m above datum on the Mary Bay crater wall, it descends to about 13 m above datum on the east side of the Fishing Bridge peninsula, and descends to 9 m across the peninsula.

On the Fishing Bridge peninsula, the *S5* shoreline truncates an extensive fill terrace of Pelican Creek (Fig. 10). This terrace postdates *S5.5,* because this shoreline is not developed on the terrace but is present on both sides (Figs. 5, 10). A narrow valley of a small stream was eroded into this Pelican Creek terrace, but it abruptly terminates at the *S5* shoreline (Fig. 10). This incised valley and the Pelican Creek bench into which it is incised must have extended farther south to a lower lake level than the *S5* shoreline. Lake level then rose (Fig. 4), and bluff erosion by the *S5* shoreline truncated the stream valley.

***S5.5* Shoreline-**. The *S5.5* shoreline is a double- crested barrier beach that extends from Mary Bay to Pelican Creek. Hydrothermal explosion deposits from the MBII event mantle the shoreline terrain of Mary Bay to within at least 1 km of Pelican Creek (Fig. 10; see also Fig. 13). This mantle extends from just above *S5* across *S5.5* to above *S6*. The *S5.5* barrier beach shows up clearly through this mantle about 1 km east of Pelican Creek, where field measurements indicate that the explosion deposits are more than 1 m thick. Eastward towards the Mary Bay source, the MB II explosion deposit thickens until it completely obscures the *S5.5* barrier beach about 0.5 km west of the crater rim (Fig. 10).

Shoreline *S5.5* becomes totally obscured within 1 km of the valley of Pelican Creek (Fig. 10), apparently by a diamicton locally exposed at the top of Pelican Creek banks. The source and mode of deposition of the diamicton is unclear, but we speculate that it originated in a hydrothermal explosion up Pelican Creek and the explosion debris formed a debris flow that spread deposits over the lower valley.

The correlation of *S5.5* is less certain west of Pelican Creek, because *S5.5* is eroded out or buried by the extensive bench along Pelican Creek above the *S5* shoreline on the Fishing Bridge peninsula. Northwest of this terrace, *S5.5* may correlate to a possible wave-cut scarp east of the Yellowstone River that has a tilt sub-parallel to that of *S5* (Figs. 5, 10, 12). An age for *S5.5* of ~13.6 ka is estimated based on shoreline sequence and the relation of the MBII deposits that mantle *S5.5* to Glacier Peak ash.

***S6* Shoreline-.** *S6* is best expressed just east of Pelican Creek with a well-defined 3-m high wave-cut scarp (Fig. 10). Farther east, a mantle of hydrothermal explosion deposits obscures it. Assuming an age of about 13 ka for the MBII explosion deposit that mantles both *S6* and the next lower *S5.5*, we estimate that S6 is ~14-14.5 ka.

3B2. Possible lake level culminations near 2.5 and 4.5 ka

From the present *S1* time back to the abandoning of *S2* about 8 ka, the northwest part of Yellowstone Lake has been near or below its present level. From 3-4 ka, lake and river levels were ~5-6 m below present, but several lines of evidence suggest the lake was near its present level (*S1* shoreline) ~2.5 and ~4.5 ka (Fig. 4). We find rationales for either of two possible lake-level histories between 6 ka and 1 ka (Fig. 4). The possible culminations near 2.5 and 4.5 ka have some data in their support, but require rather rapid changes in lake level.

Behind the modern barrier beach just east of the mouth of Pelican Creek, charcoal dating 2.7 ka (2,550 ± 60 yr. BP, 94P33, Table 1, #1) was collected at the base of 1.65 m of eolian sand and 25 cm above beach gravels. During or following deposition of these beach gravels ~1 m above datum, Pelican Creek entered the lake to the east of this site. It has subsequently established its inlet west of this site. Rising lake levels to the present shoreline would facilitate this change near 2.5 ka. In addition to the Pelican Creek site, the sandy part of the fine-grained section in the core from the drowned Yellowstone River (Fig. 6) contains wood 2.37 m below datum with an age of 2.7 ka (2,518 ± 100 yr. BP; Table 1, #2), indicating a river level somewhat below present. In an adjacent core, an age of 2.7 ka (2,560 ± 70, Table 1, #3) beneath the sand suggests a maximum age for the sand and possible level of Yellowstone River near present.

In the recently uplifted Storm Point geothermal center, slabby openwork platform gravels 3.43 m above datum contain charcoal 2.1 ka (2,160 ± 60 yr BP, Table 1, section A, not numbered). This uplifted beach here is distinct from the modern beach, *S1*, and also appears to indicate a culmination a little older than 2 ka.

About halfway from Lodge Point to the outlet, a barrier beach (Fig. 5) with a clearly developed soil occurs at the same level as modern storm deposition, including that from high water of 1996 and 1997. The soil has a 12-cm thick color B-horizon, and four, 1-cm thick clay lamellae at depths between 12 and 35 cm, consistent with an age of several millennia. The soil is buried by 35 cm of modern beach deposition, particularly that of 1996 and 1997. A projectile point recovered from this beach in the collections at the Yellowstone Museum at Mammoth (FS#1911) is of the Hanna type. This Northern Plains projectile point style was originally defined by Wheeler (1954) and represents a Middle Archaic

index artifact dating between 4500 and 2800 yrs BP (Greiser 1986), suggesting a calibrated age in the 4 ± 1 ka range.

In eastern Mary Bay north of Holmes Point, a shoreline within 1 m of modern high water but with tree cover, significant soil development, and obsidian artifact flakes may also indicate a lake level near present, several thousand years old but younger than 8 ka.

5a. Summary of Post-glacial lake level chronology.

Figure 4 plots the history of Yellowstone Lake and River level changes in the northern Yellowstone Lake area over the last ~15,000 yr. Both *S5.5* and *S6* are older than the ~13 ka MBII explosion deposit and estimated to be about ≈ 13.6 and 14.4 ka. Shorelines *S6* and *S5.5* are younger than ice-cap deglaciation of the Yellowstone Lake and plateau area. Above the Yellowstone delta area (Fig. 2), Richmond and Pierce (1972) note that a very prominent 60-65 foot shoreline (~18-20 m) at Beaverdam Creek correlates by outwash relations with late Pinedale mountain valley glaciation, somewhat younger than an age of 14.7-16.3 ka (13,140 ± 700 yr BP, Richmond and Pierce, 1972, section 14; Porter and others, 1983, Table 4-7, E). Locke and Meyer (1994, Fig. 4), however, surveyed the shoreline elevation at this locality to 27.6 m (90 feet) above datum, and correlated it with their *S9* shoreline. We note that *S7* in the Southeast Arm may correlate with S5 in northern Yellowstone area, because the LIDAR imagery shows that *S5* adjacent to Pelican Creek traces to *S7* of Locke and Meyer (1994) near Mary Bay.

Radiocarbon ages from the Yellowstone Lake area suggest that deglaciation had occurred by 16.2 ka (>14,000 yr BP, Porter and others, 1983; Whitlock, 1993). At time of the Deckard Flats readjustment, the icecap on the Yellowstone Plateau had greatly receded but was probably still present (Pierce, 1979; Sturchio and others, 1994). The radiocarbon chronology of deglaciation is several thousand years older than that produced by cosmogenic surface-exposure dating, which places the Deckard Flats readjustment at ~13.8 ± 0.4 ka (Licciardi and others, 2001). We cannot resolve why cosmogenic ages are younger than radiocarbon ages, but suggest either one or both dating systems may be in error.

S5 is estimated to be ≈ 12.6 ka as bracketed as younger than the ≈ 13 ka MBII explosion deposit and older than the ≈ 10.7 ka *S4* (Fig. 4). *S4* was constructed about 10.7 ka, as dated by Cody Complex projectile points and a ^{14}C age. Subsequent formation of the S-meander indicates a relatively low lake level about 2 m above present at ~9.5 ka. *S3* is incompletely preserved and is not well dated, but was formed after initial drowning of the S-meander and before formation of *S2*. *S2* is the best-dated shoreline at ~8.0 ka based on multiple ages on both sides of the outlet.

After formation of the *S2* shoreline at about 8.0 ka, lake levels have been below or near the present level (Fig. 4). Lake level was ~4 m below datum from 3-4 ka. Two options are shown for lake levels immediately before and after 3-4 ka (Fig. 4). (1) A gradual lowering to 3-4 ka followed by a gradual increase to present. (2) Possible culminations near the present level ~4.5 ka and ~2.5 ka that bracket low between 3 and 4 ka and with lows both before ~4.6 ka and after 2.2 ka. Both histories are shown with

question marks in that present information may be interpreted to favor either option. Either option after ~2 ka is consistent with the historic rise of LHR relative to the outlet at a rate of about 4 mm/yr (Fig. 4).

5b. Uplift of Le Hardys Rapids (LHR) indicated by submerged localities.

Table 3 shows calculations of the uplift of Le Hardys Rapids to sites in the lake and to the outlet by normalizing localities to the outlet based on the 1923-76 uplift dimensions. These calculations indicate between 8 and 9 m uplift of the Le Hardys Rapids relative to the outlet following the low stand 3-4 ka (Table 4, line 10). Uplift of LHR relative to the Bridge Bay and Little Thumb Creek North sites is calculated to be 10.2 and 11.1 m, respectively (Table 3, line 9). Normalization of these sites to the outlet based on the 1923-76 uplift pattern yields values of 8.2 and 8.6 m, similar to the 8.5 calculated for the outlet (Fig. 6) . From the low stand at 3-4 ka to the present, the net rate of uplift is less than the historic rate from 1923-75 (Table 3, compare #11 to #12), although this does not consider a possible high stand near 2 ka and possible submergence after that as shown in the option in Figure 4. Uplift or subsidence of LHR relative to the outlet is only about one-quarter of the total uplift and subsidence relative to the areas beyond the caldera margin (Fig. 1). These rates of ~3-4 mm/yr, if extended to the caldera margin and multiplied by 4, would be 12-16 mm/yr. This is within the range of 16 mm/yr for the 1923-85 uplift as well as for other calderas such as Campi Flegrei, Italy, where rates of 10-20 mm/yr have been observed over millennial time scales. (Dvorak and Mastrolorenzo, 1991). In a compilation of data for more than 100 calderas worldwide showing signs of unrest, Newhall and Dzurisin (1988) found rates of uplift and subsidence of tens of mm to greater than 100 millimeters per year.

4. Faulting.

Late-Quaternary faulting has broken many parts of the Yellowstone Plateau, especially outside of the caldera, but locally within it as well (Christiansen, 2001, Machette and others, 2001). Because of high thermal gradients and shallow young intrusions within the caldera, the brittle-ductile transition may lie at a depth of only 3-5 km, limiting faulting to shallow crustal levels. Compared to sites where the brittle-ductile transition is at about 15 km, maximum earthquakes are of lesser magnitude (Smith and Braille, 1993). In contrast to the large subsided half-graben basins and uplifted blocks of adjacent Basin-and-Range terrain (e.g., Jackson Hole and the Teton Range), normal fault systems in the caldera have little net offset, and commonly form grabens and fissure-like structures.

The Elephant Back fault system is the most prominent set of young faults within the caldera, and strikes northeasterly from the Sour Creek resurgent dome to east of the Mallard Lake dome (Fig. 1). This fault zone is nearly parallel to the caldera long-axis, which also forms the axis of historical uplift and subsidence. The faulting of the Elephant Back system may result from general extension, or from fracturing and keystone faulting associated with localized doming along the caldera axis. These young faults cut the 150 ka Elephant Back flow, but leveling resurveys of benchmarks across the northeast end of the Elephant Back zone show no apparent steps or offsets suggesting faulting since the first survey in 1923 (Dzurisin and others, 1994, Dan Dzurisin, spoken commun., 1995).

LIDAR imagery reveals a fault that offsets post-glacial surfaces across the west tip of the Fishing Bridge Peninsula and extends 3 km to the NNE (Fig. 5). Figure 14 shows local shoreline profiles, shoreline tilts, and fault offset, which are tabulated in Table 2. Only shorelines *S2* and the barrier beach

of *S4* are preserved actually crossing the fault. *S2* and the *S4* barrier beach at the east end of the Fishing Bridge peninsula are actually higher than their upfaulted remnant at the west end of the Peninsula (Fig 14), although farther eastward *S2* and *S4* are horizontal (Fig. 12). The ratio of fault offset to total shoreline elevation difference across the Fishing Bridge peninsula produced by tilting into the fault is about 60% (Table 2, S2 and BB S4). Two methods were used to estimate offset of wavecut *S4* and *S5* which do not cross the fault. One is based in the fault offset equaling 60% of the tilt into the fault (Table 2. The other method was a visual projection of the shoreline across the fault (Fig. 14) consistent with shoreline west of the fault (Fig. 12). Table 2 outlines the sequence of tilting and surface-offset faulting events.

We infer that a faulting event occurred between erosion of the *S4* wave-cut shoreline and construction of the *S4* barrier beach on the Fishing Bridge peninsula. Faulting and subsidence of the hanging wall apparently submerged the west end of the wave-cut *S4* shoreline. Longshore drift of sediment from Pelican Creek then prograded a barrier beach across the south side of the drowned area to form a lagoon. Because the strongly tilted *S4* wave-cut shoreline and much less tilted *S4* barrier beach are at the same elevation on the east side the Fishing Bridge peninsula (east side of Fig. 14), lake level did not change significantly before construction of the barrier beach, and faulting did not affect the lake outlet level. The *S4* interval is the only time during the period of shoreline terrace formation that a barrier beach and lagoon existed on the Fishing Bridge peninsula. This relationship also links the time of tilting and offset with barrier beach and lagoon formation.

Features in the area of the S-meander are also offset by the Fishing Bridge fault (Figs. 5, 8). A *S2* sand spit built across the S-meander is offset 1.8 m. The higher bench just south of and older than the S-meander is offset 1.2 m (Fig. 5), indicating no increase in offset going back to at least the ~9.7 ka age of the S-meander. Figure 8 shows that the gradient of the channel of the S-meander is ~0.9 m/km along most of the meander. No other fault strands offset the wide belt occupied by the S-meander. Farther north, a Yellowstone River terrace that predates the S-meander is offset 1.5-1.8 m by the Fishing Bridge fault (Fig. 5). The fault continues northward with surface offsets of 1 m or less, and dies out above the *S6* shoreline. Surfaces older than the ~9.7 ka S-meander on both sides of the Yellowstone River are offset less than 2 m.

A ~1 km-wide graben is located on the floor of Yellowstone Lake 0.5 km SE of the Lake Hotel (Fig. 2). Seismic reflection profiles by Otis and others (1977) first revealed this graben, and Kaplinski (1991) mapped it in greater detail. Because of its potential involvement in shoreline deformation, Locke and Meyer (1994) termed this structure the Outlet graben. However, recent detailed mapping with GPS control (Morgan and others, submitted; Johnson and others, submitted) shows that it is about 1 km west of where originally mapped and has a more northwesterly strike. The primary fault on the west side of the graben strikes about N 10° W from the north end of Stevenson Island (Figs. 1, 10). Because it does not appear to intercept the outlet, we call this fault the Lake Hotel fault. No faulting of shorelines has been observed in the Lodge Bay area, but along the lakeshore in Lodge Bay directly below the Hamilton Store parking lot (Fig. 10), vertical fractures with 10-20 cm openings in compact “lacustrine till” suggest extensional deformation, possibly due to lateral spread. Directly above these fractures, *S5* platform

gravels at 10-11 m above datum are not offset. Farther north along this trend, the Lake Hotel fault may extend onshore to a prominent escarpment behind the Lake Lodge and that continues northward to the outlet area. No evidence of offset of surface sediments has been observed in the field or with LIDAR data, however, and the *S5* barrier beach adjoins this escarpment, but is not offset (Fig. 5). Therefore, any fault offset on this escarpment is older than *S5* and in *S5* time this was a wave-cut cliff.

Local deformation of shorelines.

LIDAR data defines a strong local tilting away from the Storm Point geothermal center (Fig. 15). The shorelines that intersect the center (*S2*, *S1.8*, and *S1.6*) show steep subparallel tilts of as much as 6 m/km. The shorelines that skirt north of the center show lesser tilting; *S4* shows a gentle 4-m-high dome, and *S5* is apparently not affected. This tilting resembles Holocene bulges on the floor of Yellowstone Lake inferred to be related to hydrothermal pressures (Johnson and others, submitted).

A local dome just east of Pelican Creek has about 3 m relief in *S3* and *S4* (Fig. 15), and is also well-defined in adjacent minor shorelines (Fig. 10). Shorelines on the east limb of the dome form a sharp "v" fold with the shorelines tilted away from the Storm Point hydrothermal center (Figs. 15, 10). We have observed no hydrothermal features or faulting in the immediate vicinity, but this dome implies sub-surface pressure buildup, and merits additional investigation to understand the cause of deformation and any associated hazard. South of the anticline, the beach sands on the shore of Yellowstone Lake are hot at a shallow depth and the site of a rare thermophilic(?) sand verbena, *Abronia ammophila* (Whipple, 2001). This may reflect hydrothermal processes associated with the anticline. Younger shoreline features in this area bury the S3 shoreline.

6. Discussion

The pattern of both rises and falls of lake level (Fig. 4) combined with the historically observed inflation and deflation suggests intriguing volcanic, hydrothermal, and/or other processes may be involved. Table 4 outlines the many processes for changing Yellowstone Lake and River levels. In the following, we discuss most of these emphasizing processes most relevant to our study. We attribute the overall decrease in lake level observed during the first half of the record to lowering of the outlet by a combination of erosion and subsidence. We suggest that a millennial-scale oscillation also occurs superposed on the lowering during the first half of this record and is the primary signal during the second half of this record (Fig. 4). We suggest this millennial scale oscillation in lake levels in part reflects caldera-wide inflation and deflation similar to that recognized from re-leveling surveys and radar interferometry studies. Our radiocarbon and archeologically dated history (Fig. 4) provides a temporal scale two orders of magnitude longer than the historic studies. New observations of faulting and local shoreline deformation are based on LIDAR data. In addition to investigating the processes responsible for lake level change, the history itself provides a framework for archeology, including possible human habitation of both subaerial and now submerged shorelines.

A rising water level greatly enhances landward erosion and the development of wavecut shorelines, a process described by the Bruun Rule (Bruun, 1988; Schwartz, 1987). The better-developed shorelines (*S1* to S6 and higher) recognized by Meyer and Locke (1986) and Locke and Meyer (1994) appear to

have been developed under rising lake conditions as suggested by the Bruun Rule, and as discussed for the history of each shoreline in this report.

Decreases in lake level

Holocene outlet erosion and Pleistocene glacial damming (I-A and B in Table 4). Above ~ 20 m at LH, the Yellowstone River appears to have been downcutting mostly through unconsolidated glacial and alluvial material in the LHR area. Farther North in Hayden Valley, ice dammed lake sediments (pkl) are mapped to 7,800 feet and locally to 8,740 (20 m locally to 33 m above datum; LHR is ~1 m below datum). Thus Yellowstone lake levels from ~20 m and higher, or above S6 may have been dammed by recessional glaciers from the Beartooth Uplift during the Deckard Flats and younger times (Pierce, 1979).

Figure 4 shows a pattern of oscillating lake levels with a net lowering from ~20 m for *S6* at ~ 14.4 ka to about the present lake level at S-meander time about 10 ka. Assuming LHR has returned to the same vertical position for each shoreline, erosion of LHR at 4 m/kyr is indicated from 14.4 ka to 10 ka. Conversely, the change in shorelines levels may have been accompanied either by: 1) tectonic sagging of LHR, in which case the rate of erosion would be less, or 2) net uplift of LHR in which case the rate of erosion would be greater. Our correlations of shorelines from Fishing Bridge to the Mary Bay area are based on new LIDAR data and indicate a pronounced sagging, notably *S5* sags from ~18 m to ~ 10 m above datum from Mary Bay to the outlet.

Figure 4 also shows that after 10 ka, lake levels have oscillated but with no clear trend. Hamilton and Bailey (1990, Fig. 3) draw a bedrock threshold at LHR 5 m above datum. Bedrock is locally mapped to 20 m above datum on the west side of LHR (Christiansen and Blank, 1975). An erosionally resistant zone near the base of the Lava Creek Tuff forms the bedrock ledge of Le Hardys Rapids (R.L. Christiansen, spoken commun., 2002). This little-fractured, ~1-3 m thick devitrified zone is composed largely of interlocking micro-spherulites 1-3 mm across, making it quite resistant to erosion. Above this spherulite zone is a devitrified zone with joints on a decimeter scale that is more readily eroded. Below the spherulite zone, the Yellowstone River will next encounter the basal vitrophyre that is also much more fractured and also will be more readily eroded. The resistant bedrock zone appears to have been base level for the Yellowstone River for a considerable time, perhaps all of Holocene time. The ~3 ka gravel channel of the outlet reach is now below the level of this bedrock threshold. The 9.7-ka S-meander channel is drowned at its downstream end and thus projects at or below this bedrock threshold, suggesting little erosion of LHR over this time interval. The shorelines also show general sagging into this area (Fig. 12), however, so some of the low altitude of the ~9.7 ka S-meander channel is probably from this sagging. The erosion rate at LHR over the last 10 ka must be low in any case, and would be expected given the low bedload transport rate at LHR. Bedload supply in the outlet reach is limited to sand and fine gravel supplied by bank erosion and material carried to the outlet by longshore transport.

Tectonic stretching (I-D in Table 4). A crystallizing batholith probably exists beneath Yellowstone (see Christiansen, 2001 and references therein). Yellowstone is along the east margin of the Basin and Range structural province where tectonic extension is occurring. In addition, the Elephant Back fault zone offsets the 150 ka Elephant Back rhyolite flow (Fig. 5) indicating either significant SE-NW extension perpendicular to the caldera axis or keystone faulting associated with resurgent doming. Given that

ductile material is as shallow as 4-5 km beneath the caldera (Smith and Bruhn, 1984; Fournier and Pitt, 1985, Smith and Braille, 1994), tectonic extension would stretch and thin the ductile body and cause subsidence perhaps accompanied by fissuring and faulting in the brittle material above (Fig. 16,B). LHR lies along the axis of the caldera where the greatest subsidence due to extension might be expected. (See note under II-D regarding subsidence associated with convergence).

Yellowstone Lake ceasing to overflow (I-E in table 4). Hamilton and Bailey (1988) observed submerged shorelines and suggested that they might indicate that Yellowstone Lake ceased to overflow. Locke and Meyer (1994) considered that Holocene climatic change was unlikely to have caused closed basin conditions, as an average of 45% of annual precipitation in the Yellowstone Lake basin currently discharges at the lake outlet. Studies of oxygen isotopes of waters entering and exiting Yellowstone Lake suggest that about 15% of the inflow evaporates from the lake surface at present (Pat Shanks, oral commun., 2000). For Yellowstone Lake to cease overflowing, the ratio of evaporation to inflow would have to increase by more than 6 times, necessitating a major climatic change. Pollen records from the Yellowstone Lake basin do not show evidence for dramatic late Holocene vegetation and climatic changes (Whitlock, 1993; Baker, 1976; Waddington and Wright; 1974) The simplest argument against closed basin conditions is the drowned outlet channel of the Yellowstone River that now lies well below the level of the bedrock threshold farther downstream at LHR. This channel was cut 3-4 ka when Yellowstone Lake was more than 5 m below its present level yet was clearly overflowing with substantial velocity and discharge (Fig. 6).

Increases in Lake level

Inflation by magma intrusion (II-A in Table 4). Decompression melting in the mantle from the Yellowstone hotspot source is thought to generate basaltic magma that rises upward to the base of the rhyolitic magma chamber (Fig. 16A). Uplift or inflation because of magma intrusion is quite plausible (Pelton and Smith, 1982; Dzurisin and others, 1994). Modeling indicates that the historic inflation is consistent with a volume expansion involving either magmatic or hydrothermal fluids, primarily in the 3-6 km depth range (Vasco and others, 1990), or 8 km (Wicks and others, 1998). Uplift may relate either directly to this basaltic magma influx or a rhyolitic magma generated by its heat and intruded at shallow levels within the caldera.

Tectonic compression (II-D in Table 4). Local compression of a ductile magma chamber would produce uplift (Meertens and Levine, 1985). GPS studies show that radial convergence (compression?) was accompanied by subsidence, suggesting the opposite effect (Smith and others, 1997; Meertens and Smith, 1991). This pattern indicates that subsidence is caused primarily by depressurization of a subcaldera source, rather than by tectonic extension.

Possible increases or decreases in lake level

Faulting and local warping (III-A in table 4). A north-trending fault system includes the Lake Hotel fault on the lake floor and the Fishing Bridge fault (see section on faulting discussed earlier). Although the Fishing Bridge fault offsets shoreline *S5* and the wavecut shoreline of *S4* several meters, it offsets less than 2 m the ~9.7 ka S-meander and surfaces that pre-date the S-meander. The shorelines show an

overall sag across the outlet area (Fig. 12). The *S2* shoreline is dated ~8 ka on both sides of the Fishing Bridge fault and is only offset 0.5 m by the fault (Fig. 14, Table 2).

For the Lake Hotel graben, Johnson and others (submitted) recognize 7.5 m total offset on the western fault and 3.4 m offset on the eastern antithetic fault, for a net offset of 4.1 m. The lake floor is offset 2.7 m across the Lake Hotel graben, only 1.4 m less than the net offset of 4.1 m. Based on sedimentation rates, the last and by far the largest offset was 5.7 m on the western strand with a net offset of 2.9 m within the last 2 ka. We infer that such faulting dies out northward, for the 8 ka *S2* shoreline is essentially horizontal (Fig. 12) and offset only 0.5 m by the Fishing Bridge fault.

Tiller (1995) suggests faulting might be responsible for increases in lake and river level. Except for the Fishing Bridge fault, no faults with offset of shorelines have been recognized in the outlet area, including bedrock and surficial geologic maps (Christiansen and Blank, 1975, Richmond, 1977) and shoreline studies (Meyer and Locke, 1983; Locke and Meyer, 1994; Hamilton and Bailey, 1990, Pierce and others, 1996). Just east of Le Hardy Rapids, John Good and Ken Pierce found a fault scarp with ~ 1 m down-to-the-northwest offset (Fig, 5), which is opposite to that needed to raise the level of the outlet reach. The present drowned outlet channel from the outlet to LHR does not change its nearly flat gradient or wide width as it might if a young fault crossed and uplifted the river channel (Fig. 5). The submerged shoreline deposits at Bridge Bay and at Little Thumb Creek North as well as the many drowned valleys around the lake are not within any recognized graben and thus local faulting did not cause their submergence.

Based on isostatic considerations and observed altitude changes after normal faulting, extensional faulting and associated crustal thinning is expected to produce dominantly subsidence (80%) of the downthrown block and only minor uplift (20%) of the upthrown block (Barrientos and others, 1987). Because the brittle-ductile transition zone in the caldera is only 20-35% as deep as normal in the Basin and Range, extensional structures arising from horizontal extension may have less vertical structural relief and express extension through fissures and grabens.

Glacial Isostatic Rebound (III-B in table 4). During full-glacial times, the icecap on the Yellowstone Plateau exceeded an altitude of 3,350 m (11,000 ft) above Yellowstone Lake, altitude 2,357 m (7730 ft; Good and Pierce, 1996). That ice reached a thickness of about 1 km above the Yellowstone Lake basin is based on flow from the lake area to over the top of Mount Washburn (Pierce, 1979) and eastward through Sylvan Pass at such high levels that it backfilled high into the valley of Middle Creek (Richmond and Pierce, 1972). With total compensation and a upper crust of density 2.7, isostatic depression from 1-km ice (density ~0.9) would be 330 m. Because the lithosphere is likely to be warm and more ductile beneath Yellowstone, near-total compensation may be possible near the center of the load. In addition, because of this ductile material, the rate of rebound may be much greater than in continental craton areas. The thickness and load of ice above the Yellowstone Lake basin was relatively uniform (Good and Pierce, 1996), and thus near-uniform rebound is expected in the lake area, although cooler and stiffer crust is expected outside the caldera. That both inflation and deflation have taken place in both historic time as well as post-glacial time (Fig. 4), also argues against isostatic rebound. Pelton and Smith (1982),

Locke and Meyer 1994) also discussed and rejected glacio-isostatic rebound as a mechanism to explain the historic and shoreline record.

This unweighting during deglaciation of about 1 km of ice (pressure ~ 90 bars) provides a natural experiment for evaluating the hazard of volcanic eruptions. During deglaciation, pressure in magmas beneath the Yellowstone Plateau were not sufficiently high so that the 90 bar reduction in confining pressure produced an eruption. In other areas such as Hawaii (Porter, 1979), Iceland, and the "tuyas" of British Columbia, volcanic eruptions occurred through glacial ice, commonly thought to be stagnating and unloading during deglaciation.

Oscillations in Lake Level

Figure 4 shows oscillations in lake level that can be divided into two parts: (1) an oscillating lowering from >14 ka to ~10 ka to the S-meander level, and (2) oscillations near present level from 10 ka to present. The oscillating part of this pattern may be an extension of the observed 1923-1999 pattern of inflation and deflation based on re-leveling and radar interferometry studies. The time intervals and amplitudes of inferred Holocene cycles are much greater although rates are compatible.

The increase in lake level that defines the oscillations to the *S5* and *S4* shorelines is based on truncation of shorelines and valleys shown in Figures 5 and 10. The amplitude is not known, but is estimated to be at least several meters. The increase in lake level both after the S-meander and after the 3-4 ka low is estimated to be 8.3 m between LHT and the outlet. Extending farther from the caldera axis, our studies of lake level changes suggest differential uplift of ~10-11 m at localities that span ~41-43% the 1923-76 doming (Table 2); the average long-term rate from the submergence 4-5 ka to present is in the 0.7 to 1.2-mm/yr range if extrapolated to the outer margin of the 1923-75 doming.

The oscillations suggesting rises near 5 ka and 2 ka (Fig. 4) are not well established and are included as options because of evidence for a lake level near present near 2 and 4 ka. These oscillations suggest rather rapid rates of uplift and subsidence between the outlet and LHR and we are reticent to suggest such rates are established (note slopes of uplift and subsidence on Fig. 4). From 1923-85, uplift of LHR relative to the outlet was 0.25 m at a rate of 4 mm/yr; to produce 8 m uplift at this rate would take 2 kyr.

Many of the prominent erosional shorelines, especially the ones designated *S1-S5* were formed during rising lake levels most likely produced by an inflation episode. Locke and Meyer (1994) inferred that rising water levels produced by the current episode of inflation (including inflation before the historic measurement period) were probably effective in producing the prominent modern wave-cut shorelines noted around Yellowstone Lake. This process appears indicated for the major past shorelines as well.

Unrest of calderas is common (Newhall and Dzurisin, 1988). The Phlegraean Fields caldera, Italy, a smaller trachytic caldera about 15 km across, has a 5,500 year record useful for comparison of rates, amplitudes, and patterns of inflation and deflation to Yellowstone (Dvorak and Mastrolorenzo, 1991). There, Grindley (1976) charts 55 m uplift from about 3500 to 500 B.C. at about 18 mm/yr, followed by 15 m subsidence from about 500 B.C. to about 1000 A.D. at a rate of 11 mm/yr. Subsequently, about 12 m uplift led to an eruption in 1528 A.D. followed by about 8 m subsidence (from A. Parascandola, cited in Yokoyama, 1971). These values are comparable to the historical values of uplift (15 mm/yr) and subsidence (20-30 mm/yr) for the center of the Yellowstone caldera.

If the historic caldera inflation at 15 mm/yr were to continue for 1,000 to 4,000 years, uplift would total 15 to 60 m. The subaerial shorelines do not have deformation of this magnitude, and the tilts are generally towards the caldera axis rather than away from it (Fig. 12; Locke and Meyer, 1994). Table 5 compiles overall apparent tilts with distance from the caldera axis for three shorelines. We selected S2 and S4 because they are independently dated over long distances. We selected S5 because this shoreline feature has been nearly continuously mapped (Fig. 12; Locke and Meyer, 1994). S5 of this paper along the northern lakeshore is the same as S7 of Locke and Meyer (1994) on the hydrothermal explosion crater rim above Beach Springs. *S5* shows a significant tilt towards the caldera axis, and most of this occurs outside the caldera (Table 5). *S2* shows a 2-3 m tilt within the caldera towards the axis whereas *S4* shows a 1-2 m tilt away from the axis. In summary, net post-glacial tilting of shorelines shows gentle subsidence towards the axis of the caldera. One explanation for the gentle tilts is that the prominent subaerial shorelines were formed at the culmination of an inflation cycle, and they are near horizontal at present because the present shoreline may also be forming at the culmination of an inflation cycle. This has returned the older shorelines to approximately their original horizontal positions. The cumulative gentle overall subsidence towards the caldera axis might be due to magmatic cooling. Fournier and Pitt (1985) estimate subsidence of 0.6-0.7 mm/yr due to cooling; over the age of *S5* (14.6 ka), this would total 7.5 m.

Two favored explanations for record of oscillations

A nearly steady-state process with little net volume change in post-glacial time within the caldera seems to be required to produce the observed deformation history (Table 5). Inflation and deflation of the caldera in the last 100 years has been called “breathing”; we use the term “heavy breathing” for millennial-scale, larger episodes of inflation and deflation. This “heavy breathing” of the central part of the Yellowstone caldera may reflect magmatic inflation and tectonic stretching and deflation, or (our preferred interpretation) hydrothermal fluid sealing and inflation followed by cracking and deflation (Fig. 16). The many factors noted in Table 4 may be involved. Listed below are two explanations, one involving only hydrothermal processes, and the other a hybrid of volcanic and tectonic processes.

Hydrothermal inflation and deflation (IV-A in Table 4). A large, magmatically driven hydrothermal system exists principally within the 630 ka Yellowstone caldera (Fournier and Pitt, 1985; Fournier, 1989; Christiansen, 2001). At a depth of about 5 km, a seal may be created by mineral deposition and ductile flow separating a deep zone associated with crystallizing magma and fluids expelled during crystallization and in which pore pressures can approach lithostatic, from a shallower zone in which pore pressures are hydrostatic (Fournier and Pitt, 1985; Fournier, 1989). Hydrothermal pressure buildup of the confined hydrothermal fluids beneath this seal would produce uplift. Eventual rupture of the seal, perhaps during an earthquake or hydrofracturing, would permit these confined hydrothermal fluids to escape and result in subsidence, perhaps back to the original level. This mechanism could explain why even latest-Pleistocene shorelines show little net deformation, with net inflation equal to net deflation.

Fournier (1989) calculated that the volume of magmatic fluids released by magma crystallization is adequate to explain historic uplift rates. Bob Fournier (personal commun., 2002) also estimates that no more than a 10% increase in surface manifestation of geothermal fluids has occurred, but that dense

brines from beneath the ruptured seal might not be vented directly to the surface. Instead, they may be expelled laterally at depth. Friedman (this volume), however, finds that there has been a decrease in chloride representing hydrothermal heat output of about 10% since the early 1980's, near when subsidence started in 1985. Friedman also notes that years and seasons of increased precipitation also correlate with increased chloride release. We suggest that the 10 % decrease noted by Friedman might reflect the general drought that has occurred since about 1980 (Despain, personal commun., 2002) and thus does not necessarily contradict the postulate of geothermal release producing the subsidence after 1985. Dzurisin and others (1994, p. 268) note a cluster of hydrothermal and earthquake events (for example, Nagy and Smith, 1988) within and outside the caldera that may relate to the 1985 change from inflation to deflation and be associated with rupture of a deep hydrothermal seal and release of hydrothermal fluids. In this regard, it is interesting to note that the banding of vein deposits commonly noted in mineralized areas around intrusions may also indicate pulsations in the outflow of hydrothermal fluids (Fournier, 2000).

A correlation between hydrothermal explosions and associated lowering of deep, confined hydrothermal pressures might also result in lowering of LHR and lake levels. Figure 4 shows that the ages of three hydrothermal explosions do not clearly correlate with times of lake-level lowering (Fig. 4), although the dating of the explosions and lake level both have considerable uncertainty. Other explosions such as Duck Pond, Fern Lake, the subaqueous Cutthroat Crater (age ~ 8.7-14.4 ka, Johnson and others, in review) and other craters need be dated to fully evaluate this possible relation.

Inflation by magma intrusion and subsidence by other mechanisms (IV-B in Table 4).
Because Yellowstone is an active volcanic field, a magmatic explanation is obviously plausible (Pelton and Smith, 1982; Dzurisin and others, 1994). The inflation has been modeled with the largest volume expansions in the 3.0-6.0 km depth range (Vasco and others, 1990). The overall horizontality of shorelines (Table 5) indicates there has been no net doming by buildup of post-glacial intrusions. The subsidence part of the oscillation is more difficult to explain by evacuation of the emplaced magma, although the radially outward earthquake patterns may represent outward magma movements (Smith, AGU abstract). Subsidence due to tectonic stretching of ductile material, primarily of the batholithic magma chamber, is predictable given Yellowstone's location on the margin of the extending Basin and Range. The Elephant Back fault system indicates SE-NW extension that may reflect either fracturing associated with localized doming along the caldera axis or regional extension; such doming does not provide an explanation for subsidence, but regional extension does. Outside of the Yellowstone caldera, extensional basin and range faults are clearly active, including the Teton fault, the east Sheridan fault, and the Hebgen earthquake faults. Such extension might be episodic and produce subsidence of the caldera. The Eagle Bay fault has been active in Holocene time and extends from south of the caldera into it (Fig. 2).

Subsidence due to cooling is almost certainly occurring (0.6-0.7 mm/yr, Fournier and Pitt, 1985), but can account for only a small fraction of the historically observed rates of about 20 mm/yr uplift and subsidence (Dzurisin and others, 1994, Fig. 4). This suggests that cooling is a minor factor in subsidence.

If inflation is explained by magma intrusion and deflation is explained by extension or other process, the following questions are of concern: (1) why the volume of magma intrusion and associated uplift would equal the volume of extension and subsidence?, and (2) why would these alternate systematically in time?

Local doming and faulting of shorelines.

In addition to the changes in lake level, remarkable local deformation is recorded by shoreline faulting and tilting. The cause of the tilting and doming is locally associated with hydrothermal centers. For example, west from the Storm Point hydrothermal center with its dramatic craters (Fig. 10) , tilt is 6 m over a kilometer (Fig. 15). A localized anticline just east of Pelican Creek has no surface features and merits further investigation. On the lake floor, domal areas attributed to hydrothermal processes have even greater relief than these onshore sites (Johnson and others, in review). Outside of the northern Yellowstone Lake study area, Locke and Meyer (1994) show broad uplift of the Rock Point area and subsidence of the West Thumb area.

The Fishing Bridge fault shows increasing offset of older shorelines. Tilting into the fault is equal or greater than fault offset. Over a distance of about 1.1 km across the Fishing Bridge Peninsula, tilts into the Fishing Bridge fault increase from 0.8 m for *S2* to 6.7 m (projected) for *S5* (Fig. 14, Table 2).

7. Conclusions

S2 (8 ka) and related shorelines are tilted as much as 6 m in one kilometer away from the Storm Point hydrothermal center. Just west of this tilted area is a local dome more than 2 m high and about 0.5 km across. Both of these uplifts suggest shallow emplacement of a volume that is still present, presumably of magma or hydrothermal fluids. This and similar features on the lake floor and perhaps elsewhere may represent a significant hazard.

LIDAR data permits recognition of the Fishing Bridge fault and its history of Holocene offset. Near Fishing Bridge, the fault offsets *S2* 0.5 m and the *S4* barrier beach 1 m. About 2 m of faulting occurred after eroding the wave cut *S4* but before building the *S4* barrier beach. The Fishing Bridge fault 0.5-1.5 km farther north offsets by 1-2 m the *S2* sand spit filling the S-meander, but offsets less than 2 m adjacent surfaces that pre-date the S-meander, indicating offset after ~11 ka (*S4*)is the same as that after 8 ka (*S2*). Curiously, Late Holocene activity on the Fishing Bridge fault has been minimal (Table 2) whereas activity on the *offshore* Lake Hotel fault has been mostly late Holocene.

Shorelines *S2* and *S4* are correlated by independent dating from the north to south shores of the lake and are essentially horizontal, and significantly, they do not rise towards the caldera axis. Our correlation of *S5*, a well represented shoreline along the north and east side of the lake gently slopes towards the caldera axis. This overall near-horizontality contrasts with local doming and faulting of shorelines where structural relief exceeds 5 m.

We reconstruct the following post-glacial history of changes for Yellowstone Lake and adjacent areas (Fig. 4).

1. MBII hydrothermal explosion occurred about 13 ka and mantles *S5.5* and *S6*, but not *S5*. The steep crater wall on the north side of Mary Bay was formed during the MB II explosion and *S5* was cut into the crater wall.

2. Using LIDAR images, *S5* can be traced from Pelican Creek to Mary Bay where it is *S6* of Meyer and Locke (1986) and *S7* of Locke and Meyer (1994). *S5* post dates the MB II hydrothermal explosion and is ~12.6 ka.
3. The *S4* shoreline is ~10.7 ka and is 7-9 m above datum in the Fishing Bridge area and 7-8 m above datum east of Grant Village area. Locke and Meyer (1994) note local uplift of *S4* of about 4 m in the Mary Bay and Rock Point area to about 12 m above datum.
4. The S-meander represents a low level of Yellowstone Lake and LHR that occurred after the *S4* shoreline and before *S2*/*S3*. Uplift of LHR by more than 8 m relative to the outlet converted this once vigorously flowing reach of the river to an arm of the lake.
5. The *S2* shoreline is about 4-6 m above datum on both sides of the outlet, is nearly undeformed, and is ~ 8 ka by dating on both sides of the outlet.
6. Yellowstone Lake has been near or below its present level from after *S2* time ~8 ka to present.
7. About 3-4 ka inn Bridge Bay and in the drowned valley of Little Thumb Creek-North, lake level was 5.4 and 6.3 m lower, respectively, than the present *S1* shoreline. The outlet reach of the Yellowstone River is presently a drowned channel that had a much higher gradient before 3 ka. Estimation of original river gradients indicates uplift of LHR relative to the outlet was about 8 m, and thus converted this reach from a once vigorously flowing river to the present "pool".
8. Other evidence of now-submerged lake-level features is widespread but not yet dated and includes (1) drowned valleys such as Pelican Creek, Sedge Creek, and Little Thumb Creek, (2) submerged shorelines 2-4 m below datum (S^{-1}) and 10-13 m below datum (S^{-3}) noted by Johnson and others (submitted), and (3) shorelines submerged 15-30 m below datum noted by Hamilton and Bailey (1990) at many tens of locations. Better dating and correlation is needed to understand these submerged shorelines.

The overall pattern lake levels (Fig. 4) suggests an oscillating lowering of lake level from at least the *S6* level ~ 14 ka to after the *S2* level at ~ 8 ka. This is easiest to explain by erosion of the outlet accompanied by inflation-deflation cycles, however, the tilt of *S5* towards the caldera axis (Table 5) may indicate subsidence of the threshold at LHR. After *S2* time, the lake has been below of near its present level and little outlet erosion seems indicated. The increase in lake level from 3-4 ka to present (Fig. 4) can be explained by uplift of LHR.

The cyclic model suggested by historic deflation and inflation explains many aspects of the record over the last 15 kyr. In particular, it explains broad-scale net deformation of shorelines of generally less than 10 m in contrast to historical rates of uplift and subsidence of up to 1-2 cm/yr (10-20 m/1,000 yr). If shorelines were cut during intervals of rising (transgressing) lake level as suggested by Locke and Meyer (1994), the present lake level (*S1*) and shorelines *S3, S4,* and *S5* probably represent lake level culminations. This sequence of shorelines is sub-horizontal (*S2*-*S4*),or declines towards the caldera axis (*S5*) because they represent culminations of maximum uplift in an oscillation that has produced no net uplift. Because the present time appears to be a culmination, the other culminations may also appear essentially horizontal. This history and geometry supports cycles of inflation and deflation with an amplitude of about 8 m between LHR and the outlet and a frequency of perhaps1-3 ka.

For caldera inflation or deflation, several mechanisms are likely to be operating: magma intrusion, crustal stretching, batholithic cooling, and hydrothermal pressure changes. The mechanism of uplift by hydrothermal pressure buildup beneath a hydrothermal seal followed by subsidence due to rupture of the seal, and release of fluids is appealing for by itself it explains the large scale near horizontality of shorelines. Local sagging of shorelines may be explained by extension and faulting whereas local doming may result from hydrothermal or perhaps magmatic buildup. Subaerial shorelines that represent inflation culminations and relative lake-level highstands are sub-horizontal. Submerged shorelines that formed during deflation episodes and overall lower lake levels might be expected to be more tilted than shown by Johnson and others (submitted), but as suggested by the Bruun Rule, even the submerged shorelines might represent minor culminations of lake level during longer-period oscillations. That subaerial post-glacial shorelines do not slope strongly away from the caldera axis suggests that either voluminous magma intrusions have not accumulated or the uplift volume of such intrusions have been fortuitously balanced by subsidence process such as tectonic stretching or batholithic cooling. Inflation appears responsible for the lake level rises (Fig. 4), but such inflation has not resulted in volcanic eruptions or cumulative doming of shorelines with tilts away from the caldera axis. The inflation-deflation cycles seem to represent an essentially zero sum process with little net subsurface volume change, which seems most readily explained by buildup and release of hydrothermal fluids.

Hydrothermal explosions are likely associated with lowering of pressure of the confined hydrothermal system and subsidence. Wicks and others (1998) conclude transfer of fluids over 10's of km between the two resurgent domes has occurred in a few years, which would indicate that caldera scale interconnections may occur on a similar time scale. The ages of three hydrothermal explosions do not clearly correlate with times of lake-level deflation (Fig. 4) , although the dating of the explosions and lake level both have considerable uncertainty. Other hydrothermal explosion craters such as Duck Lake, Fern Lake, the subaqueous Cutthroat Crater, and other craters need be dated to better evaluate this hypothesis.

The Yellowstone caldera was covered with about 1 km glacial ice about 17-20 ka. Deglaciation and the reduction in pressure by about 90 bars was not accompanied by volcanic eruptions, suggesting the magmatic system was not then, and perhaps not now, at pressures high enough for eruption.

Acknowledgements. We appreciate the work of the crew of the Midwest Archeological center in finding archeological and charcoal material for dating, and particularly George Crothers for surveying. The Park Service staff at Lake was particularly helpful, including John Lounsbury, Dan Reinhart, Bruce Sefton, Loyd Kortge, Harlan Credit, Dan Mahony, and the NPS dive team. Kerry Cook and Dan Lofgren of the Federal Highways Administration provided records and samples from borings. We appreciate the field conferences with Bob Christiansen, Pat Muffler, Rick Hutchinson, and Wayne Hamilton. Bob Fournier greatly aided understanding of hydrothermal processes and their relation to uplift and subsidence proceses. Bob Smith provided GPS data on the ongoing deformation. Dan Dzurisin provided surveying data and advice concerning the deformation processes. Pierce particularly appreciates fieldwork together and discussions with Lisa Morgan and Pat Shanks on the lake floor and hydrothermal explosions. Bill

Locke did the definitive surveying of the shorelines and their interpretation and discussed this freely with us. Bill Locke and Dan Dzurisin provided very helpful and knowledgeable reviews.

References Cited

Baker, R. G., 1976, Late Quaternary vegetation history of the Yellowstone Lake basin, Wyoming: U.S. Geological Survey Professional Paper 729E, p. E1-E48. Cannon, K.P., Crothers, G.M., Pierce, K.L., 1994 Archeological Investigations along the Fishing Bridge Peninsula, Yellowstone National Park, Wyoming: The Archeology, Geology, and Paleoenvironment. Midwest Archeological Center, Lincoln, Nebraska, 367 p.

Barrientos, S.E., Stein, R.S., and Ward, S.N.., 1987, Comparison of the 1959 Hebgen Lake, Montana, and the 1983 Borah Peak, Idaho, earthquakes form geodetic observations: Bulletin of the Seismological Society of America, v. 77, p. 784-808.

Bruun, P., 1988, The Bruun Rule of erosion by sea-level rise: A discussion on large-scale two- and three-dimensional usages, Journal of Coastal Resources, v. 4, p 627-648.

Cannon, K.P., Crothers, G.M., and Pierce, K.L. 1994, archeological Investigations along the Fishing Bridge Peninsula, Yellowstone National Park, Wyoming: The archeology, geology and paleoenvironment. Technical Report on file, National Park Service, Lincoln, Nebraska, 367 p.

Cannon, K.P., Pierce, K.L., and Crothers , G.M., 1995, Caldera Unrest, Lake Levels, and Archeology: The View from Yellowstone Lake. Park Science v. 15, No. 3, p. 28-31.

Cannon, K.P., Pierce, L.L., and Stormberg, and MacMillian, M.V., 1997, Results of archeological and paleoenvironmental investigations along the north shore of Yellowstone Lake, Yellowstone National Park, Wyoming,: 1990-1994, Technical Report on file, National Park Service, Midwest Archeological Center, Lincoln, Nebraska,

Christiansen, R. L., 1984, Yellowstone magmatic evolution: Its bearing on understanding large-volume explosive volcanism. In Explosive Volcanism: Inception, Evolution, and Hazards, National Academy Press, Washington, D.C., p. 84-95.

Christiansen, R.L., 2001, The Quaternary and Pliocene Yellowstone Plateau Volcanic Field of Wyoming, Idaho, and Montana: U.S. Geological Survey Professional Paper 729-G, 237 ms pages.

Christiansen, R.L. and Blank H.R., Jr. 1975. Geologic Map of the Canyon Village Quadrangle, Yellowstone National Park, Wyoming, U.S. Geological Survey Geologic Quadrangle Map GQ 1192, scale 1:62,500.

Doerner, J.P. and Carrara, P.E., 2001, Late Quaternary vegetation and climatic history of the Long Valley area, west-central Idaho, U.S.A., Quaternary Research, v. 56, p. 103-111.

Dvorak, J.J., and Mastrolorenzo, Giuseppe, 1991, The mechanisms of recent crustal movements in Campi Flegrei caldera, southern Italy: Geological Society of America Special Paper 263, 47 p.

Dzurisin, Daniel, Christiansen, R.L., and Pierce, K.L., 1995, Yellowstone--restless volcanic giant: U.S. Geological Survey Open-File Report 95-59, Volcano Hazards Fact Sheet, 2 p.

Dzurisin, Daniel, Savage, J.C., and Fournier, R.O., 1990, Recent crustal subsidence at Yellowstone caldera, Wyoming: Bulletin of Volcanology, v. 52, p. 247-270.

Dzurisin, Daniel and Yamashita, K.M., 1987, Vertical surface displacements at Yellowstone Caldera, Wyoming, 1976-1986: Journal of Geophysical Research, v. 92, No. B13, p. 13,753-13,766.

Dzurisin, Daniel, Yamashita, K.M., and Kleiman, J.W., 1994, Mechanisms of crustal uplift and subsidence at the Yellowstone caldera, Wyoming: Bulletin of Volcanology, v. 56, p. 261-270.

Fournier, R.O., 1989, Geochemistry and dynamics of the Yellowstone National Park hydrothermal system: Ann. Rev. Earth Planet. Sci., v. 17, p. 13-53.

Fournier, R.O., 2000, Hydrothermal processes related to movement of fluid from plastic into brittle rock in the magmatic-epithermal environment: Economic Geology, v. 94, p. 1193-1212.

Fournier, R.O., and Pitt, A.M., 1985, the Yellowstone magmatic-hydrothermal system: *in* Claudia Stone, editor, Geothermal Resources Council, International Symposium on Geothermal Energy, International Volume, p. 319-327,

Frison, G.C., 1991, Prehistoric Hunters of the High Plains. Academic Press, New York.

Frison, G.C., 1992, The Foothills-Mountains and the Open Plains: The Dichotomy in Paleoindian Subsistence Strategies Between Two Ecosystems. In Ice Age Hunters of the Rockies, edited by D.J. Stanford and J.S. Day, pp. 323-362. University Press of Colorado, Niwot, Colorado.

Friedman, Irving, and Norton, D.R., this volume, Is Yellowstone loosing its steam?: Chloride flux out of Yellowstone National Park: U.S. Geological Survey Professional Paper ____.

Good, J.D., and Pierce, K.L., 1996, Interpreting the Landscapes of Grand Teton and Yellowstone National Parks, Recent and Ongoing Geology: Grand Teton National History Association, 58 p. 57 illus., 2nd printing, 1998.

Greiser, S.T., 1986, Artifact Collections from Ten Sites at Canyon Ferry Reservoir: Archeology in Montana, v. 27, No. 1-2, p. 1-190.

Grindley, G.W., 1976, Relation of volcanism to earth movements, Bay of Naples, Italy, in Gonzales-Ferran, O., ed., Proc. Symp. On Andean and Antarctic Volcanology problems: Rome, IAVEC, p. 598-612.

Hamilton, W.L., and Bailey, A.L., 1990, Holocene deformation history of the Yellowstone caldera at Yellowstone Lake inferred from abandoned shorelines and sediments: Yellowstone Physical Sciences Laboratory, Yellowstone National Park, Report 90-3, 24p. including 13 figures, (draft of 8 June, 1990).

Hamilton, W.L., 1987, Water level records used to evaluate deformation within the Yellowstone caldera, Yellowstone National Park: Journal of Volcanology and Geothermal Research, v. 31, p. 205-215.

Hamilton, W. L., and A. L. Bailey, 1988, Holocene deformation deduced from shorelines at Yellowstone Lake, Yellowstone caldera, I: Historical summary and implications, Eos Trans. AGU, v. 69, n. 44, p. 1472.

Husted, W.M., and Edgar, R., 2002, The Archeology of Mummy Cave, Wyoming: An Introduction to Shoshonean Prehistory. Midwest Archeological Center Special Report No. 4, and Southeast Archeological Center Technical Report Series No. 9, National Park Service, Lincoln, Nebraska. Manuscript on file at the Midwest Archeological Center, Lincoln, Nebraska.

Johnson, S.Y., Stephenson, W.J., Morgan, A.L., Shanks, W.C., III, and Pierce, K.L., submitted, Postglacial geologic processes in northern Yellowstone Lake, Wyoming., Bulletin of the Geological Society of America.

Kaplinski, M.A., 1991, Geomorphology and geology of Yellowstone Lake, Yellowstone National Park, Wyoming: M.S. Thesis, Northern Arizona University, 82 p.

Licciardi, J.M., Clark, P.U., Brook, E.J., Pierce, K.L., Kurz, M.D., Elmore, D., and Sharma, P, in press, Cosmogenic ^{3}He and ^{10}Be chronologies of the northern outlet glacier of the Yellowstone ice cap, Montana, USA: submitted to QR or Bull GSA.

Locke, W.W., l986, Shoreline elevation data for the roaded portion of Yellowstone Lake shore, Quaternary Evolution of the Yellowstone Region, Friends of the Pleistocene, Rocky Mountain Cell, Guidebook, p. 52.

Locke, W.W., Meyer, G.A. and Pings, J.C., 1992, Morphology of a post-glacial fault scarp across the Yellowstone (Wyoming) caldera margin and its implications: Bulletin of the Seismological Society of America, v. 82, p. 511-516.

Locke, W.W., and Meyer, G.A., 1994, A 12,000-year record of vertical deformation across the Yellowstone Caldera margin: The shorelines of Yellowstone Lake: Journal of Geophysical Research, v. 99, No. B10, p. 20.079-20.094.

Machette, M.N., Pierce, K.L., McCalpin, J.P., Haller, K.M., and Dart, R.L., 2001, Map and data for Quaternary faults and folds in Wyoming: U.S. Geological Survey Open File Report 01-461, map and 155 p.

Mehringer, P.J., Jr., Sheppard, J.C., and Foit, F.F., Jr., 1984, The age of the Glacier Peak tephra in west-central Montana: Quaternary Research, v. 21, p. 36-41.

Meertens, C.M., and Levine, J., 1985, Compressive tectonic strain as a possible mechanism for long-term vertical deformation of the Yellowstone caldera: EOS, Transactions of the Americana Geophysical Union, v. 66,, no. 46, p. 853.

Meertens, C.M., and Smith, R.B., 1991, Crustal deformation of the Yellowstone caldera from first GPS measurements: 1987-1989: Geophysical Research Letters, v. 18, p. 1763-1766.

Meertens, C.M., Smith, R.B., and Puskas, C.M., 2000, Crustal deformation of the Yellowstone caldera from campaign and continuous GPS surveys, 1987-2000: EOS, Transactions, American Geophysical Union, v. 78, No 46, p.

Meyer, G.A., 1986, Morphology of the Yellowstone River below the nominal lake outlet at Fishing Bridge and topographic map of the Lake Lodge area. Quaternary Evolution of the Yellowstone Region, Friends of the Pleistocene, Rocky Mountain Cell, Guidebook, p. 47-49.

Meyer, G.A., and Locke, W.W., 1986, Origin and deformation of Holocene shoreline terraces, Yellowstone Lake, Wyoming: Geology, v. 14, p. 699-702.

Morgan, L.A., Shanks, W.C., and others, submitted, new maps of the floor of Yellowstone Lake, submitted to Science

Muffler, L.J.P., White, D.E., and Truesdale, A.H., 1971, Hydrothermal explosion craters in Yellowstone national Park: Geological Society of America Bulletin, v. 82, p. 723-740.

Nagy, W.C., and Smith, R.B., 1988, Seismotectonic implications of the 1985-86 Yellowstone earthquake swarm from velocity and stress inversion: Seismological Research Letters, v. 59, p. 20.

Newhall, C.G., and Dzurisin, Daniel, 1988, Historic unrest at large calderas of the World: U.S. Geological Survey Bulletin 1855, 2 volumes, 1108 pages!

Otis, R.R., Smith, R.B., and Wold, R.J., 1977, Geophysical surveys of Yellowstone Lake, Wyoming: Journal of Geophysical Research, v. 82, p. 3705-3717.

Pelton, J.R., and Smith, R.B., 1979, Recent crustal uplift in Yellowstone National Park: Science, v. 206, p. 1179-1182.

Pelton, J.R., and Smith, R.B., 1982, Contemporary vertical surface displacements in Yellowstone National Park: Journal of Geophysical Research, v. 87, No. B4, p. 2745-2761.

Pierce, K.L., 1979, History and dynamics of glaciation in the northern Yellowstone National Park area: U.S. Geological Survey Professional Paper 729F, 91 p.

Pierce, K.L., Cannon, K.P., and Crothers, G.M., 1994, Archeological Implications of Changing Lake Levels of Yellowstone Lake, Yellowstone National Park, Wyoming. Current Research in the Pleistocene, v. 11:106-108.

Porter, S.C. 1979, Hawaiian glacial ages: Quaternary Research, v. 12, p. 161-187.

Porter, S.C., Pierce, K.L., and Hamilton, T.D., 1983, Late Pleistocene glaciation in the Western United States, *in* Porter, S.C., ed., The Late Pleistocene, v. 1, *of* Wright, H.E., Jr., ed., Late Quaternary Environments of the United States: Minneapolis, Minn., University of Minnesota Press, p. 71-111.

Reeve, S.A., 1989, Prehistoric Settlements at the Yellowstone Lake Outlet, Yellowstone National Park, Wyoming. Manuscript on file at the Midwest Archeological Center, Lincoln, Nebraska, 161 p.

Reid, J.B., Jr., 1992, The Owens River as a tiltmeter for Long Valley caldera, California: The Journal of Geology, v. 100, p. 353-363.

Richmond, G.M., 1973, Surficial geologic map of the West thumb quadrangle, Yellowstone national Park, Wyoming: U.S. Geological Survey Misc. Geol. Inv. Map I-643.

Richmond, G.M., 1974, Surficial geologic map of the Frank Island quadrangle, Yellowstone national Park, Wyoming: U.S. Geological Survey Misc. Geol. Inv. Map I-642

Richmond, G.M., 1977, Surficial geologic map of the Canyon Village quadrangle, Yellowstone national Park, Wyoming: U.S. Geological Survey Misc. Geol. Inv. Map I-652.

Richmond, G.M., 1976, Surficial geologic history of the Canyon Village quadrangle, Yellowstone National Park, Wyoming, for use with Map I-652: U.S. Geological survey Bulletin 1427, 35 p.

Richmond, G.M., and Pierce, K.L., 1972, Surficial geologic map of the Eagle Peak quadrangle, Yellowstone National Park and adjoining area, Wyoming: U.S. Geological Survey Misc. Geol. Inv. Map I-637.

Schwartz, M. L., 1987, The Bruun Rule - twenty years later, Journal of Coastal Resources, v. 3, , p. ii-iv.

Shortt, Mack W., 2001, The Osprey Beach Site: A Cody Complex occupation on the south shore of West Thumb: 6th Biennial Scientific Conference on the Greater Yellowstone Ecosystem, abstracts, p. 37.

Smith, R.B., and Braile, L.W., 1993, Topographic signature, space-time evolution, and physical properties of the Yellowstone-Snake River Plain volcanic system: the Yellowstone hotspot, in

Snoke, A.W., Steidtmann, J.R., and Roberts, S.M., editors, Geology of Wyoming: Geological Survey of Wyoming Memoir No. 5, p. 694-754.

Smith, R.B., and Bruhn, R.L., 1984, Intraplate extensional tectonics of the western U.S. Cordillera: inferences on the structural style from seismic reflection data, regional tectonics and thermal-mechanical models of brittle-ductile deformation: Journal of Geophysical Research, v. 89, p. 5733-5762.

Smith, R.B., Meertens, C.M., Lowry, A.R., Palmer, Randy, and Ribe, N.M., 1997, Evolution and active processes of the Yellowstone Hotspot: EOS, Transactions, American Geophysical Union, v. 78, No. 46, p. F801.

Sturchio, N.C., Pierce, K.L., Murrell, M..T., and Sorey, M.L., 1994, Uranium-series ages of travertines and timing of the last glaciation in northern Yellowstone area, Wyoming-Montana: Quaternary Research, v. 41, , p. 265-277.

Tiller, C.C., 1995, Postglacial sediment stratigraphy of large lakes in Greater Yellowstone: scenarios of tectonic and climatic forcing: M.S. Thesis, University of Minnesota, Minneapolis, MN., 193 p.

Vasco, D.W., Smith, R.B., and Taylor, CL, 1990, Inversion for sources of crustal deformation and gravity change at the Yellowstone caldera: Journal of Geophysical Research, v. 95, No. B12, p. 19,839-19,856.

Waddington, J.C.B., and Wright, H.E., Jr., 1974, Late Quaternary vegetation changes on the east side of Yellowstone Park, Wyoming: Quaternary Research, v. 4, p. 175-184

Wheeler, R.P., 1954, Two New Projectile Point Types: Duncan and Hanna Points. Plains Anthropologist, No. 1, p. 7-14.

Whipple, J.J., 2001, Yellowstone sand verbena: A Yellowstone Lake endemic, 6th Biennial Scientific Conference on the Greater Yellowstone Ecosystem, Yellowstone Lake, Hotbed or Chaos or Reservoir or Resilience?, Oct. 8-10, 2001, Yellowstone National Park, Wyoming, p. 17.

Whitlock, Cathy, 1993, Postglacial vegetation and climate of Grand Teton and southern Yellowstone National Parks: Ecological Monographs, v. 63, No 2, p. 173-198

Wicks, Charles Jr., Thatcher, Wayne, and Dzurisin, Daniel, 1998, Migration of fluids beneath Yellowstone Caldera inferred from satellite radar interferometry: Science, v. 282, p. 458-462.

Yokoyama, I., 1971, Pozzuoli event in 1970: Nature, v. 229, p. 532-534

Figure Captions

Figure 1. Map showing Yellowstone National Park, the Yellowstone caldera, Yellowstone Lake and River, and contours on the historic dome of uplift from1923-75, after Pelton and Smith (1982). Uplift is primarily within the Yellowstone caldera and the axis of uplift extends between the Sour Creek and Mallard Lake domes. Note that upstream from Le Hardys Rapids (LHR) such uplift also raises the level of the Yellowstone River and Lake, and thus ties the level of Yellowstone Lake to uplift and subsidence at LHR.

Figure 2. Map of the Yellowstone Lake area, including some important localities and ages outside the LIDAR area. LIDAR data (Figs. 5, 10) covers the north shore from near the Lake Hotel (LH) to Mary Bay. Lake-floor surveys (Morgan and others, this volume) suggest a zone of faulting and fissuring connects the Holocene Eagle Bay fault (Locke and others) in the southern lake area with the Lake Hotel graben.

Figure 3. Vertical surface displacements measured by repeated first-order leveling surveys along a traverse from Lake Butte (d = 0) north-northwestward across the floor of Yellowstone caldera to Canyon Junction (d = 44 km). The traverse was measured in 1923, 1975-77 (labeled 1976 in the plot), each year from 1983 to 1993, 1995, and 1998. Shown here are the net displacements of benchmarks along the traverse for 3 overlapping time periods: 1976-1984, 1984-1985, and 1984-1992. The uplift profile for 1976-1984 is essentially the mirror image of the subsidence profile for 1984-1992, which suggests a common source region, and a remarkable unity of the uplift and subsidence processes. The transition from uplift to subsidence occurred during 1984-1985, when the observed surface displacements were negligibly small.

Figure 4. Reconstruction of changes in Yellowstone Lake level over the last 15 ka. Shoreline elevation is relative to gage at Bridge Bay Marina and for the northern lake area. Radiocarbon ages and their conversion to calendar ages are given in Table 1.

Figure 5. LIDAR image showing the low gradient “outlet reach” of the Yellowstone River from the outlet to past Le Hardys Rapids. The Outlet Reach has a gradient of only 0.25 m over a distance of more than 4 kilometers. Sand deposition along the outlet reach indicates the gradient has been diminishing and the channel becoming straighter. F- Fishing Bridge fault; S-meander- line crossed by bars. LIDAR shown with artificial illumination from the west. Shoreline symbols the same as in Figure 10.

Figure 6. Drowning of the outlet reach of the Yellowstone River after 3 ka. Note that gravel at core site is below the bedrock threshold at Le Hardys Rapids. The present drowned profile (upper horizontal wavy line) is compared to a reconstructed profile ~3 ka when gradient is estimated to have been 1m/km to the bedrock threshold at LHR (sloping line, see text). At ~3 ka, the outlet reach of the Yellowstone River was a vigorous, gravel transporting, bank-eroding stream.

Figure 7. Cross-section across the S-meander showing location of channel gravels, ~9.2 ka charcoal, and *S3* (5.5 m) and *S2* (4.1 m) shorelines. This section is based on 4 nearly connected trenches across the paleochannel labeled "Trench" in Fig. 5.

Figure 8. Profile section of the S-meander based on LIDAR data. Location shown by line with single cross-hatch in Figure 5. The meander was drowned, starting by ~9.2 ka, and invaded by Yellowstone Lake, including the *S2* sand spit ~ 8 ka. The Fishing Bridge fault has offset this sand spit ~1.8 m. The eolian sand dune filled the upper end of the S-meander when the present drowned channel was more active about 3 ka (see Fig. 5). The thalweg of the S-meander has a consistent gradient of about 1 m/km across its entire length except for where it is offset by the Fishing Bridge fault. The S-meander thalweg now descends below the surface of the outlet reach at the downstream end of the S-meander.

Figure 9. Comparison of outlet reach during S-meander time (~9.7 ka and gradient of 1m/km) with that during formation of *S3/S2* shorelines (8.6-8.0 ka). The S-meander was converted from a relatively vigorous stream carrying gravel and undercutting its steep banks (Fig. 5) to an arm of Yellowstone Lake.

Figure 10. LIDAR image of the northern lakeshore area showing shorelines *S2-S6* as well as unlabeled intermediate shorelines. Artificial illumination of LIDAR data from the north. Note surface texture of MB II explosion deposit northeast of Mary Bay. tv- truncated valley, ts- truncated shorelines.

Figure 11. Drawings of projectile points from shorelines on the north shore of Yellowstone Lake. A, B, and C, are Cody complex points (~ 9.8-10.7 ka) on *S4* deposits on the Fishing Bridge peninsula. D and E are Late Pleistocene-Early Holocene (9,000-10,000 yr BP = ~10- 11.4 ka?) stemmed points similar in age to Cody Complex from the *S4* paleolagoon. F is a mid Holocene side-notched point, (5,500-6,000 yr BP = ~6.6-7 ka?) from the *S2?* barrier beach that encloses the Beach Springs lagoon. It had been weakly abraded by either wind blown sand or wave action.

Figure 12. LIDAR profiles of northern Yellowstone Lake shorelines *S2-S6*. The LIDAR elevation of the mapped shorelines was projected at a 10 m spacing onto line ABC. *S2* is about 8.0 ka, *S4* is about 10.7 ka, and *S5* is about 12.6 ka. In the outlet area, there is a general sag and the Fishing Bridge fault. Westward from the Mary Bay crater wall at Beach Springs, the *S5.5* shoreline is mantled with a decreasing thickness of MB II deposits (open arrow symbol). The *S5* shoreline is mantled with Indian Pond explosion deposits whose thickness was measured at the position of the arrows black arrows. Note local doming associated with the Storm Point geothermal center and smaller dome just east of Pelican Creek (open arrows).

Figure 13. LIDAR profile along *S5.5* barrier beach mantled by MB II hydrothermal explosion deposit. Profile on barrier beach between X and Y on Figure 10. The barrier beach would be smooth (See Figs. 14, 15), but the explosion deposit has a surface texture with a one-meter amplitude over a 100 m distance. The increase in elevation to the east results from an increase in thickness of

MBII deposits, perhaps supplemented by tilting away from the source in the Mary Bar explosion crater.

Figure 14. LIDAR profiles showing faulting and tilting of shorelines across the Fishing Bridge peninsula. Location along line of projection between B and C on Figure 10. Four shoreline profiles indicate increased deformation from *S2* to *S5* time (see Table 2). The fault does not cross the *S4* or *S5* shorelines, but they show increasing tilt towards the fault with age. *S2* is offset 0.5 m. The *S4* barrier beach is faulted 1 m but slightly older wavecut *S4* is projected to be offset ~3.2 m, suggesting about 2 m offset during *S4* time (see text).

Figure 15. LIDAR profiles of *S4, S2* and two younger shorelines (*S1.8* and *S1.6*) from the Storm Point geothermal center west to Pelican Creek. Location along line of projection between D and E on Figure 10. The shorelines rise as steeply as 6 m in 1 km to the Storm Point geothermal center. A local anticline locally interrupts this westward tilt and is well shown by *S4* and *S3* just west of Pelican Creek. East of 1400 m, the *S 1.6* profile is not a shoreline, but a topographic profile showing the craters of the Storm Point hydrothermal center.

Figure 16. Cartoon showing mechanisms for inflation and deflation of the caldera (only some mechanisms are diagramed). A, Intrusion of magma and uplift; B, Extension of crust and contained magma body resulting in subsidence above magma body; C, Geothermal pressure buildup below seal and uplift; and D, Geothermal pressure release with rupture of seal and deflation (C and D after Fournier, written commun., 1997).

Tables

Table 1. Carbon-14 and other ages associated with levels of Yellowstone Lake, grouped by relation to shorelines, and generally in order of increasing age. (Table 1, HB-C-14.doc).

Table 2. Offsets on the Fishing Bridge fault and associated tilting across the Fishing Bridge peninsula based on offset shorelines and shoreline projections shown in Figure 14.

Table 3. Submerged Yellowstone Lake and River levels, and their normalization to the outlet.

Table 4. Processes for decreases, increases, and oscillations in Yellowstone Lake and River level in post-glacial time. The pattern of historic changes and the present drowned "outlet reach" of the Yellowstone River suggest changes in the elevation of Le Hardys Rapids are important.

Table 5. Change in elevation of *S2*, *S4*, and *S5* from outside the caldera, near the caldera margin, and nearest the caldera axis. These are remarkably similar, and if anything appear to become lower towards the caldera axis, particularly the oldest shoreline, *S5*.

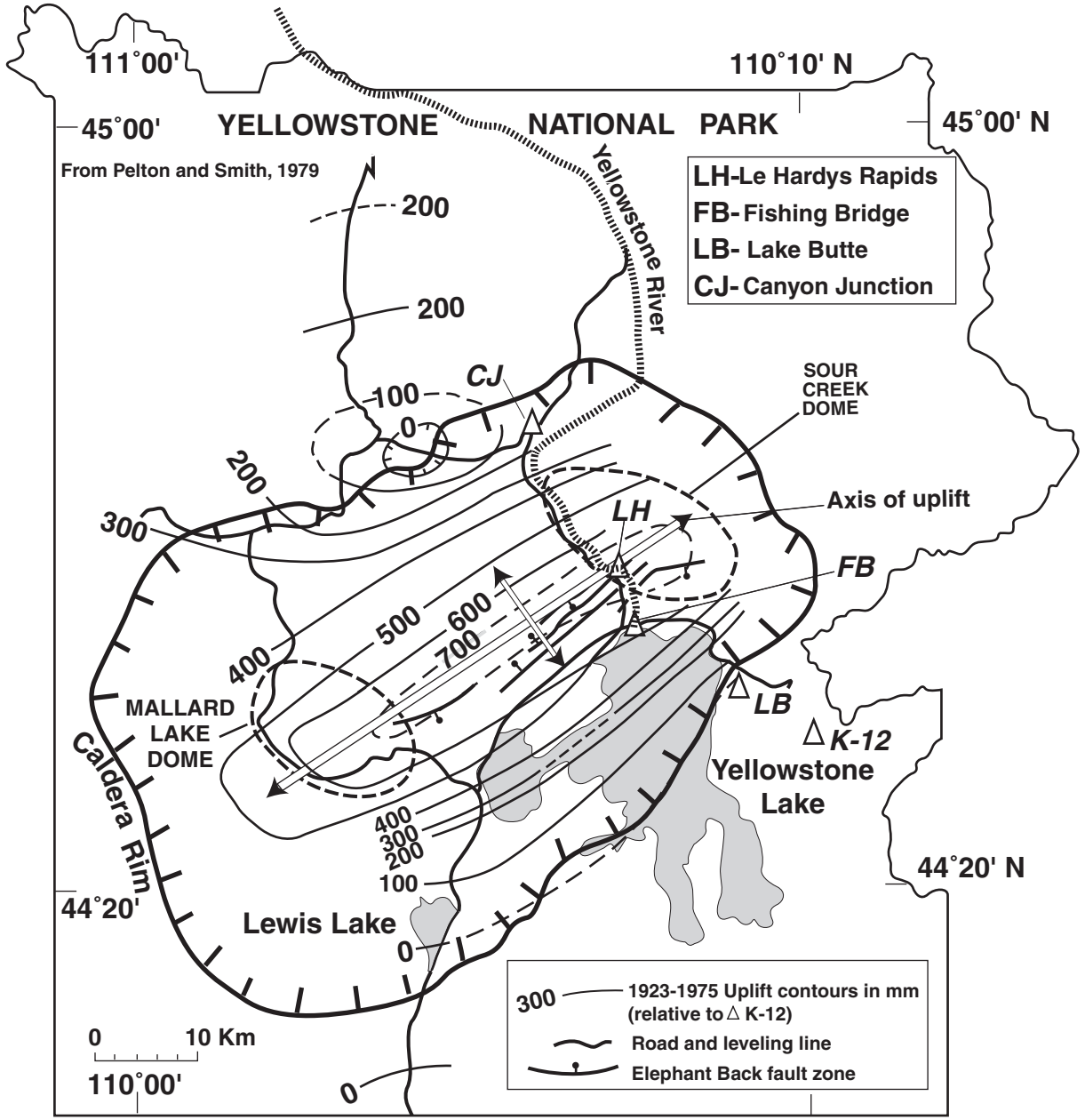

Figure 1, **(HB,Fig_1_Uplift_Dome1923-75.ai)**

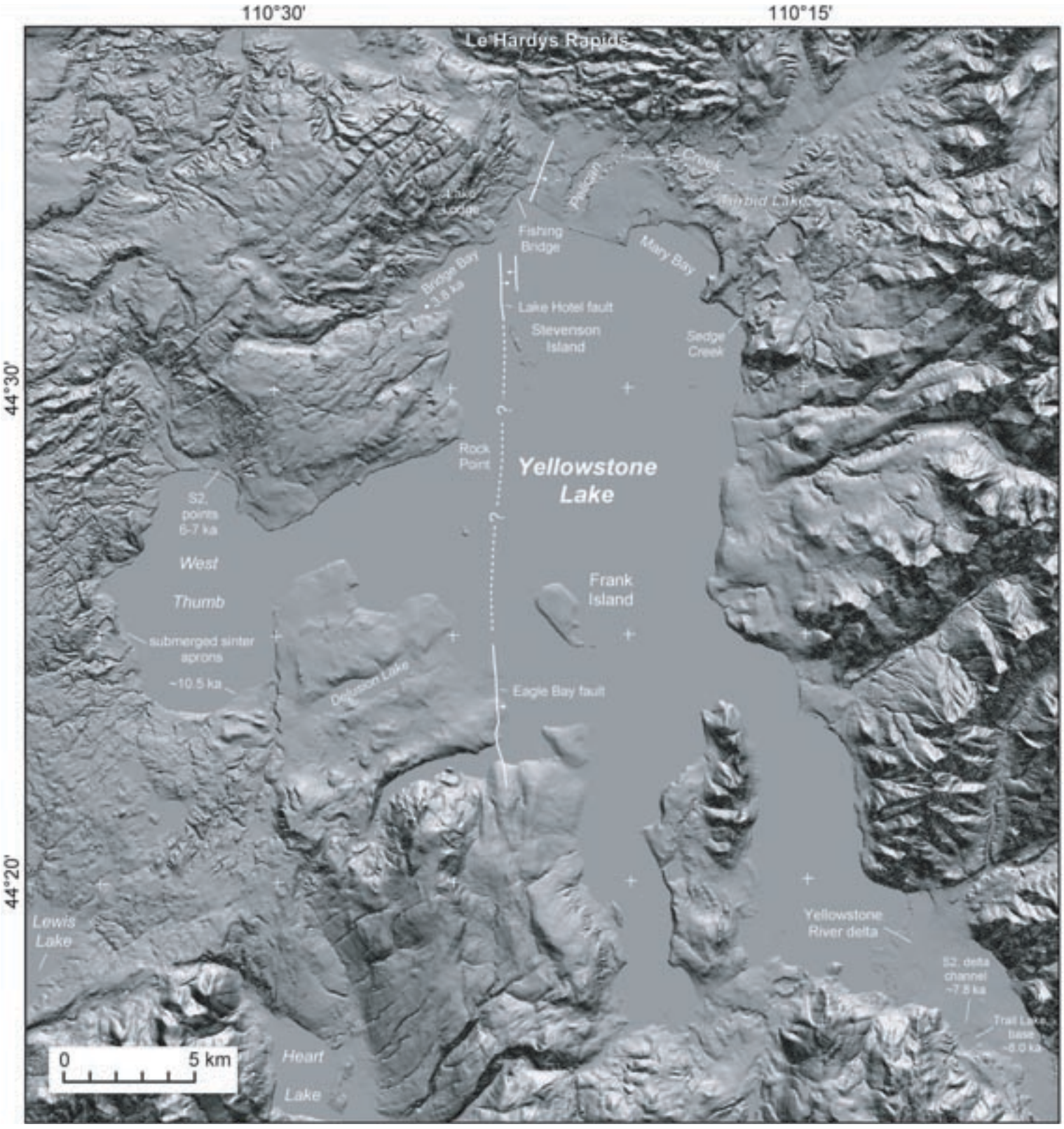

Fig 2 study area, Meyer.ai

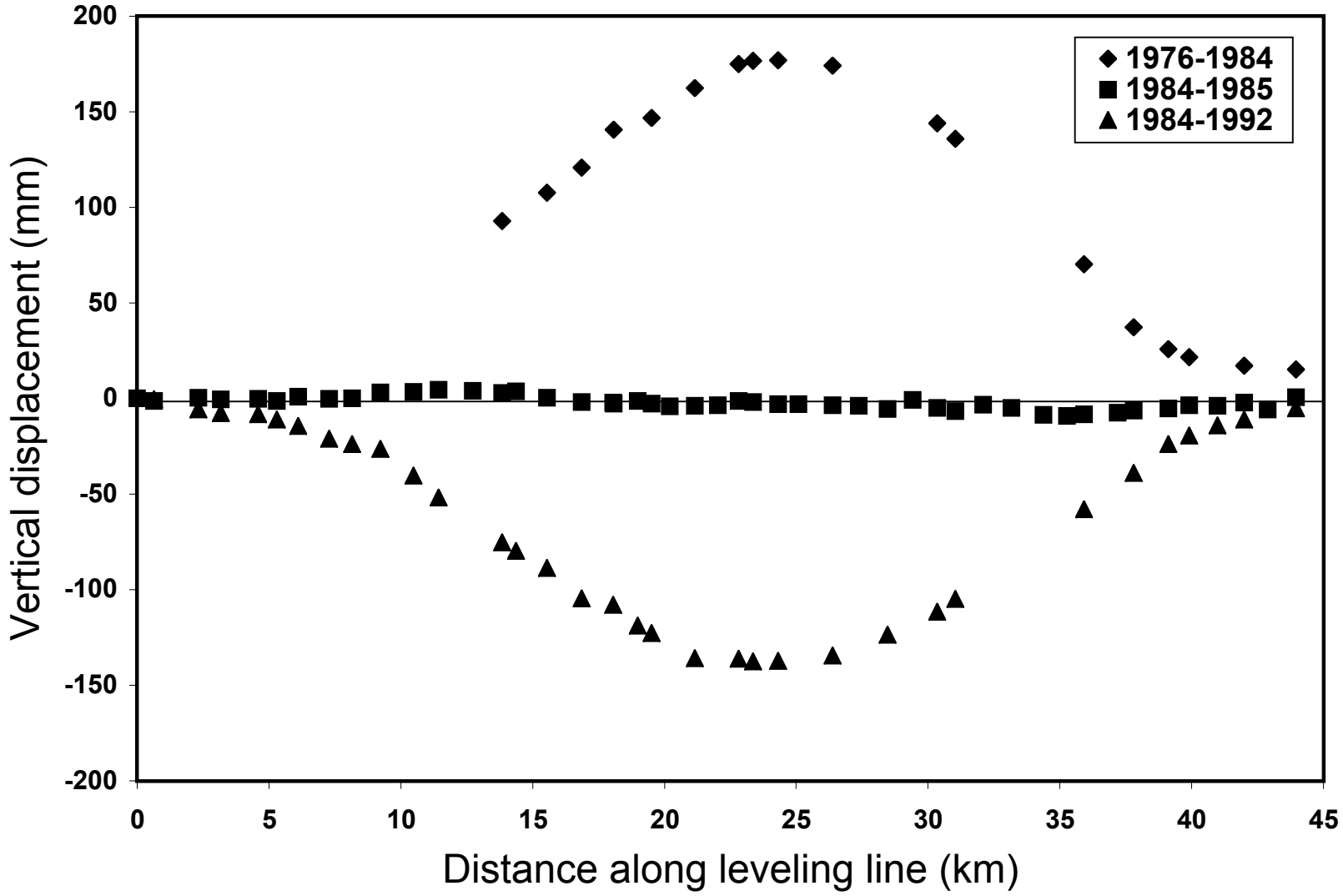
1976-1984
1984-1985
1984-1992
Vertical displacement (mm)
200
150
100
50
0
-50
-100
-150
-200
0
5
10
15
20
25
30
35
40
45
Distance along leveling line (km)

Figure 3

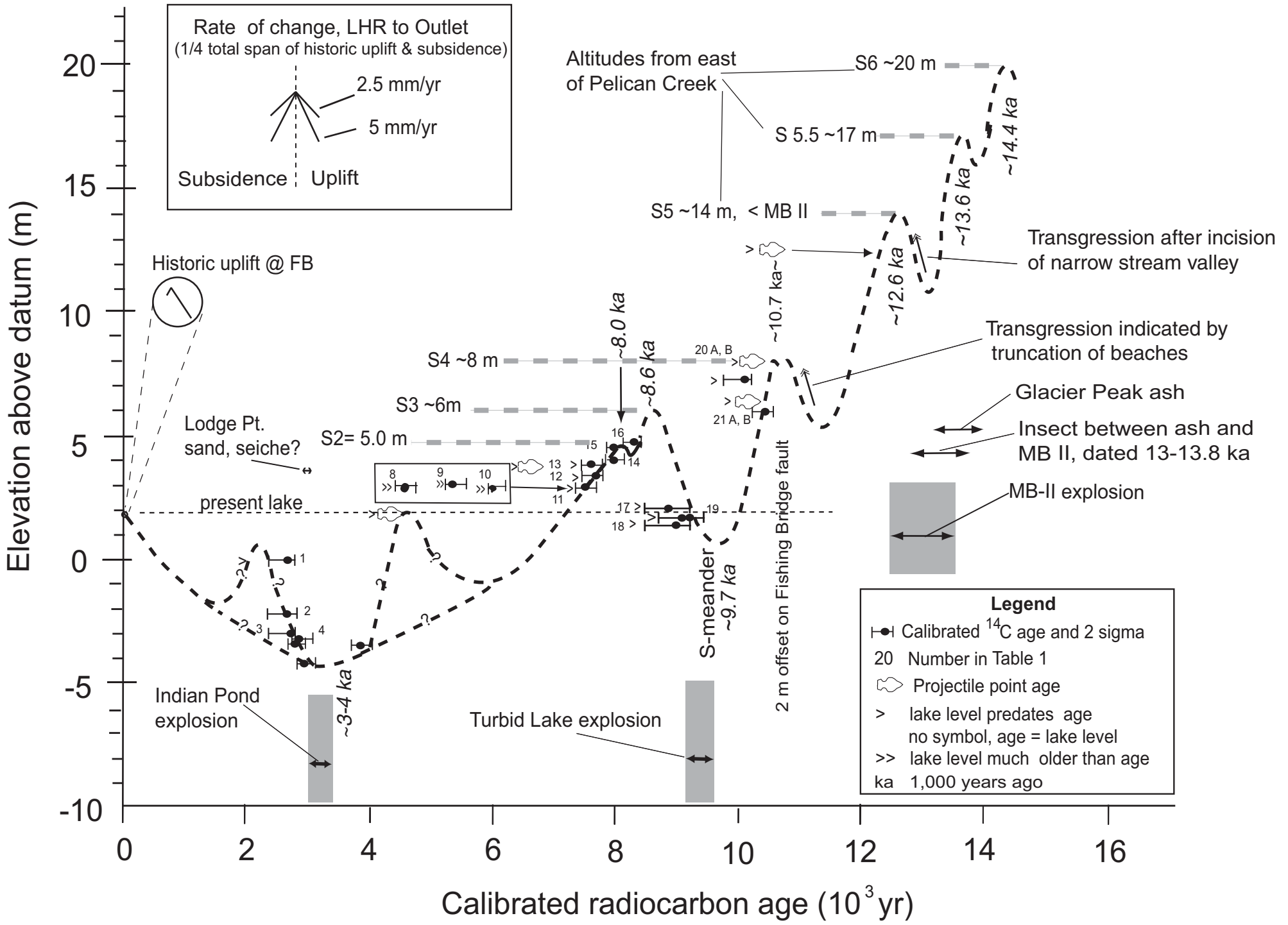

Figure 4 (HB_Figure 4_YellLakeLevelHistory.ai)

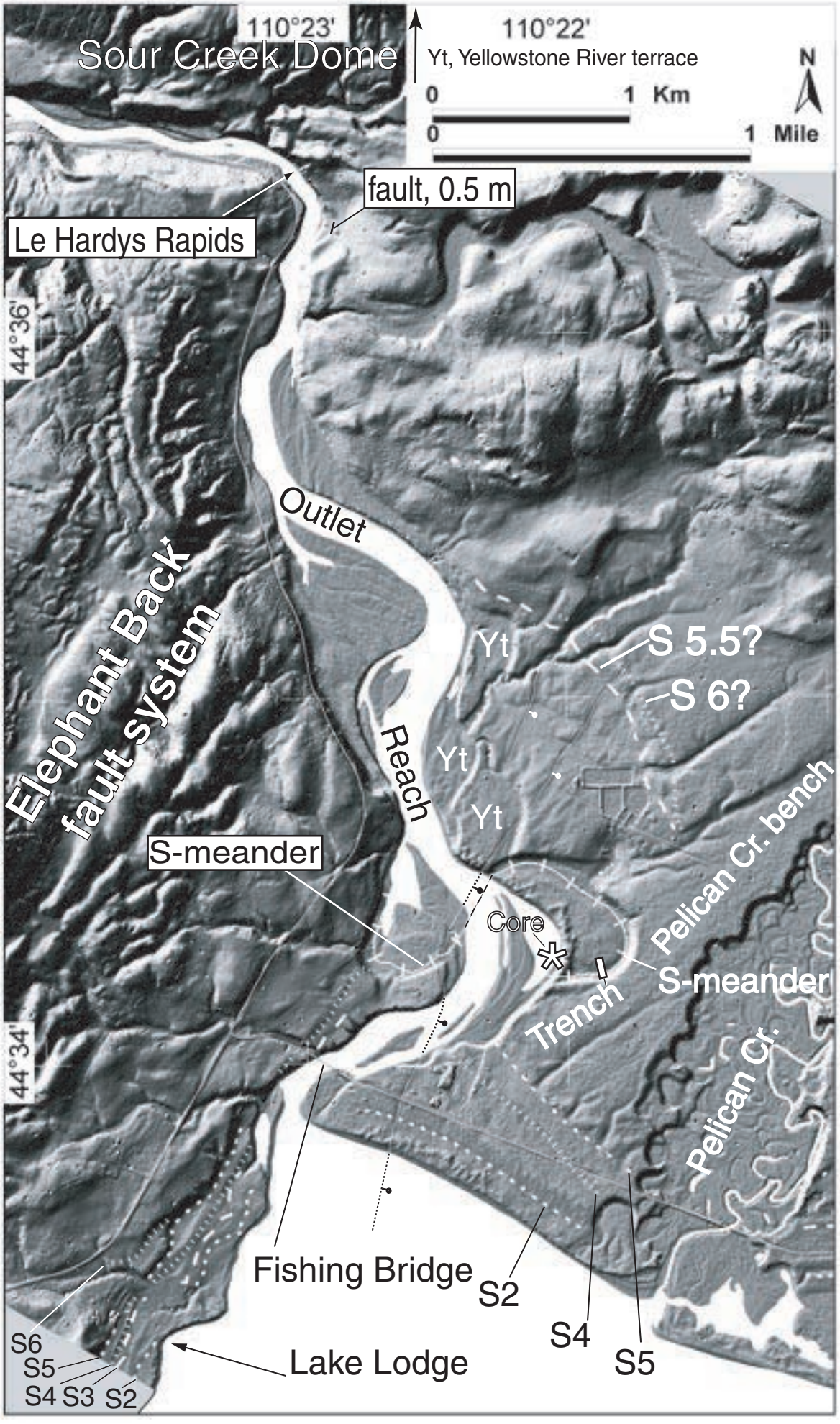
110°23'
Sour Creek Dome
110°22'
Yt, Yellowstone River terrace
0
1 Km
0
1 Mile
N
fault, 0.5 m
Le Hardys Rapids
44°36'
Outlet
Elephant Back
fault system
Yt
S 5.5?
S 6?
Reach
Yt
Yt
S-meander
Core
Pelican Cr. bench
S-meander
Trench
Pelican Cr.
44°34'
Fishing Bridge
S2
S4
S5
S6
S5
S4 S3 S2
Lake Lodge

Figure 5

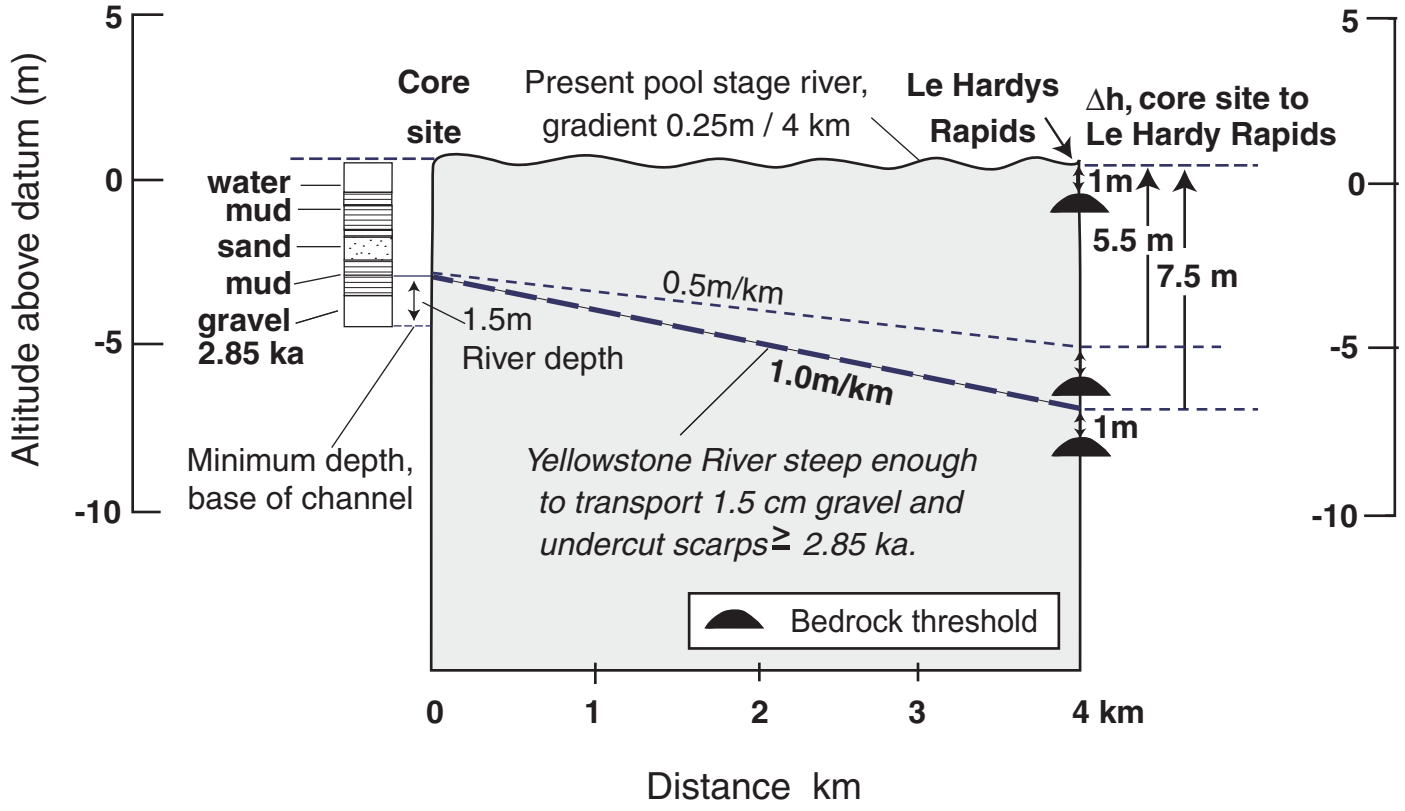

Figure 6 (HB_Fig 6_3 ka to present)

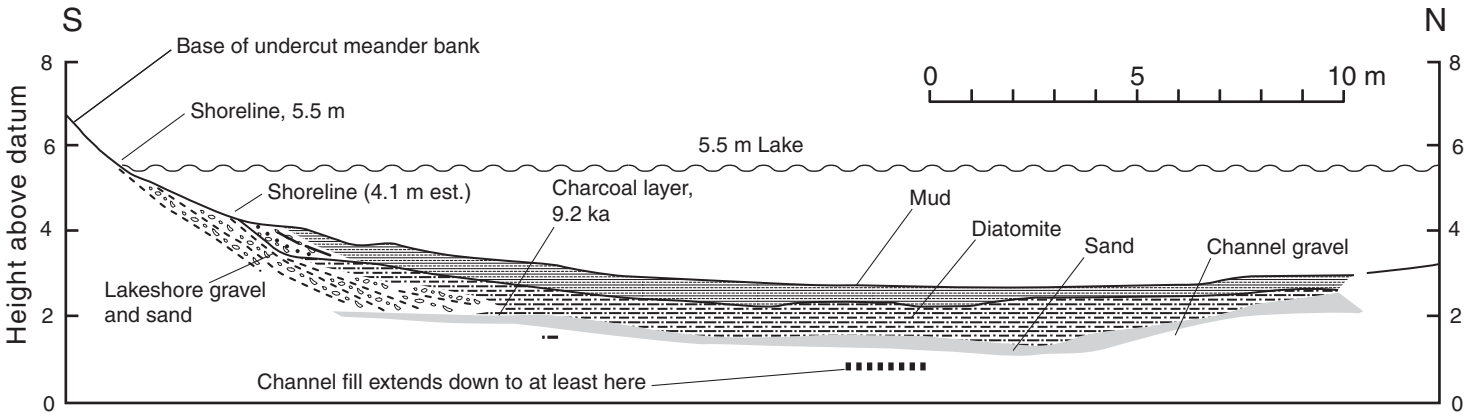

Figure 7 (HB_Fig7_xsection_meander.ai)

Figure 8, (Fig8_S-meander Profile)

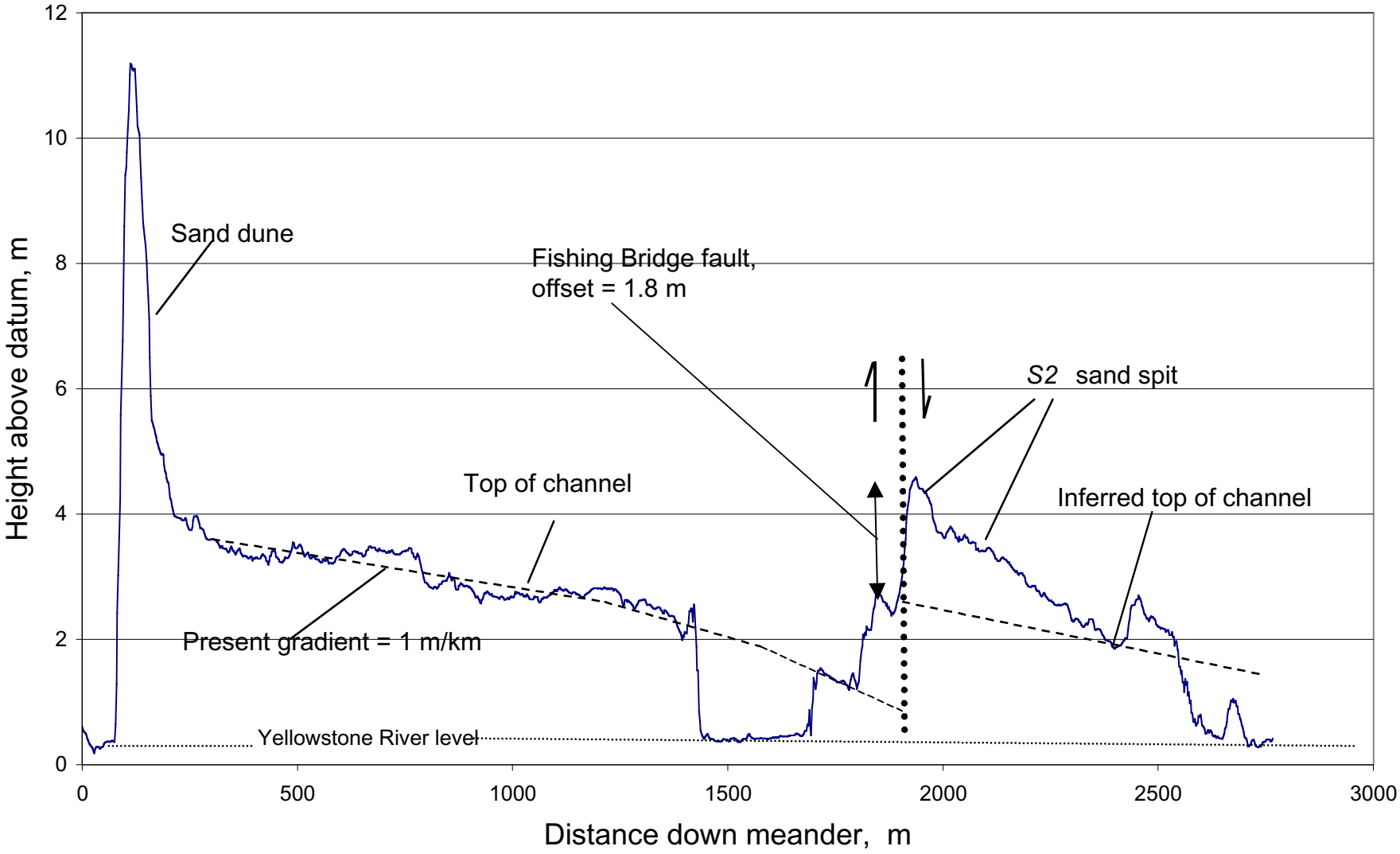

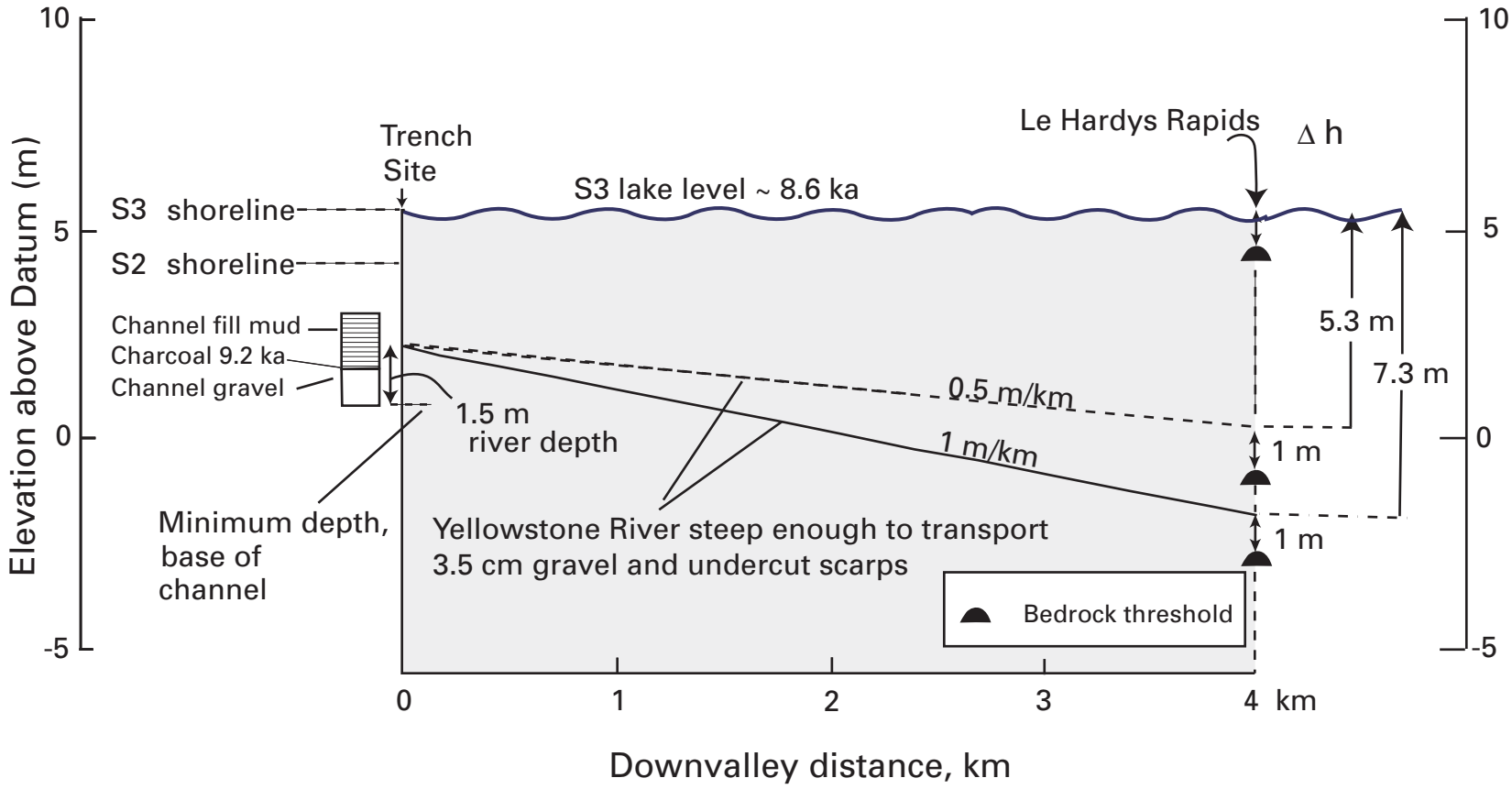

Figure 9 (Fig9, S-Meander drowning.ai)

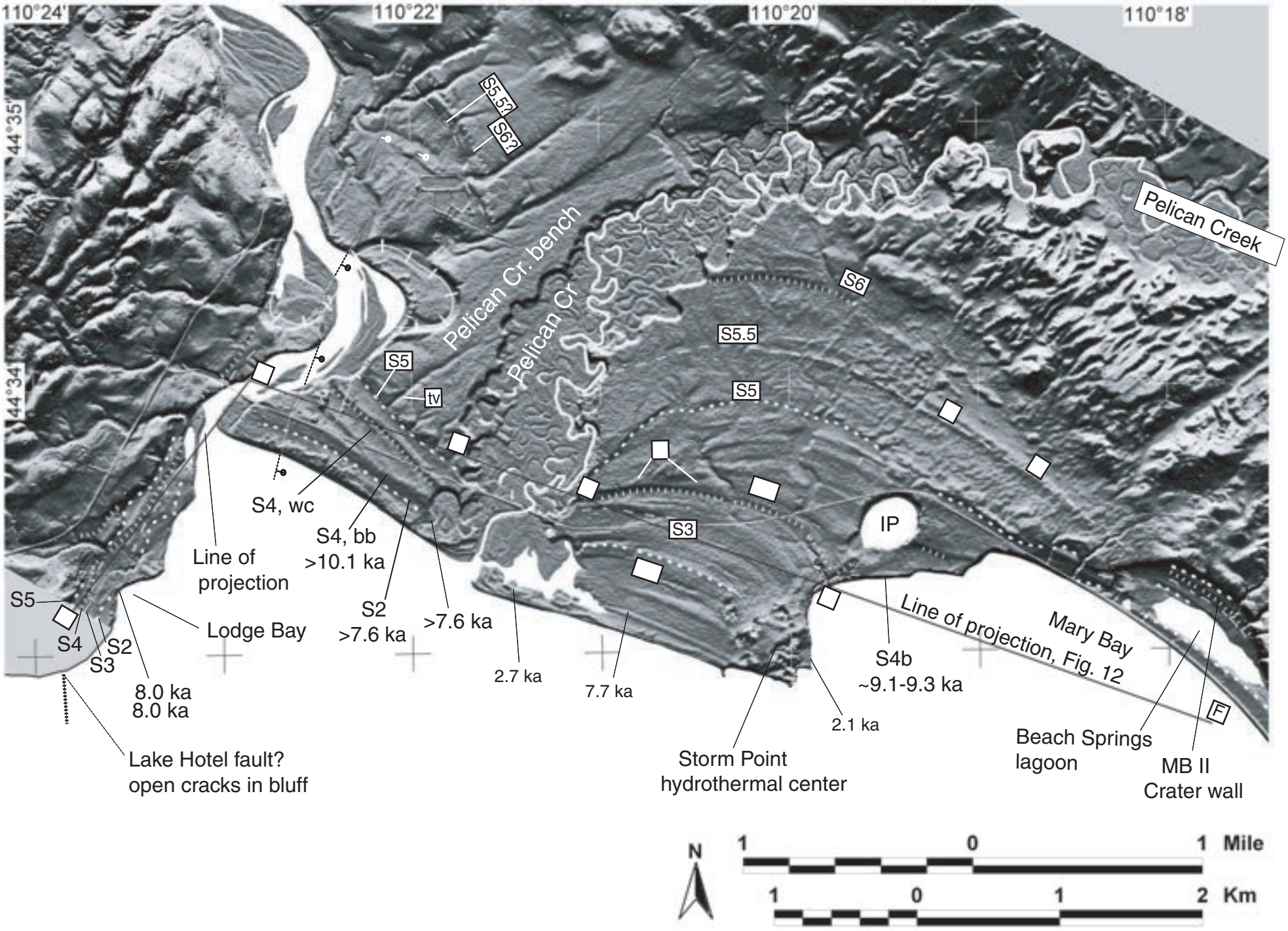

Figure 10 (HB_Fig10_LIDARnorth_shorelines.ai)

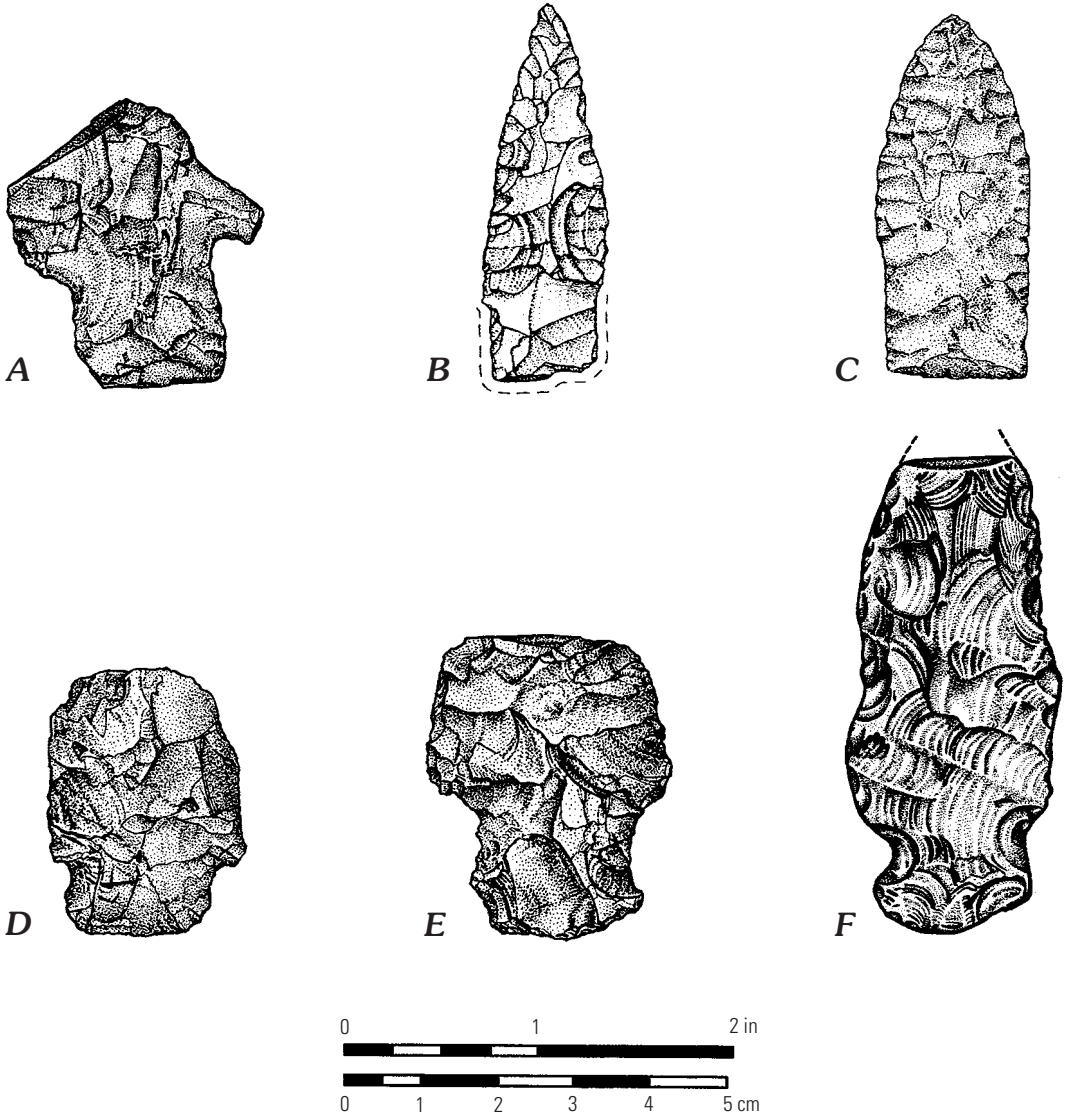

Figure 11

Figure 12 (Fig12_S profilesLIDAR

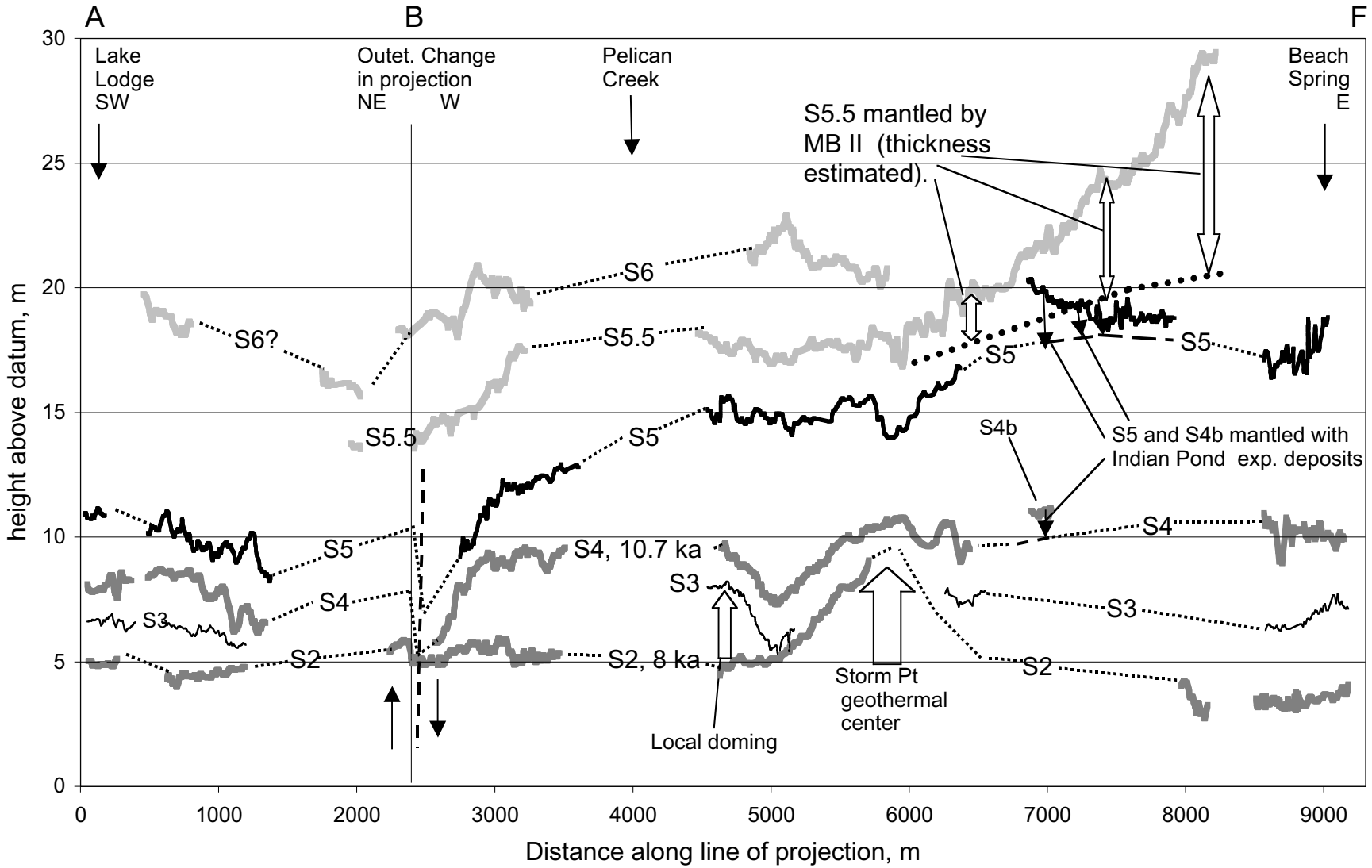

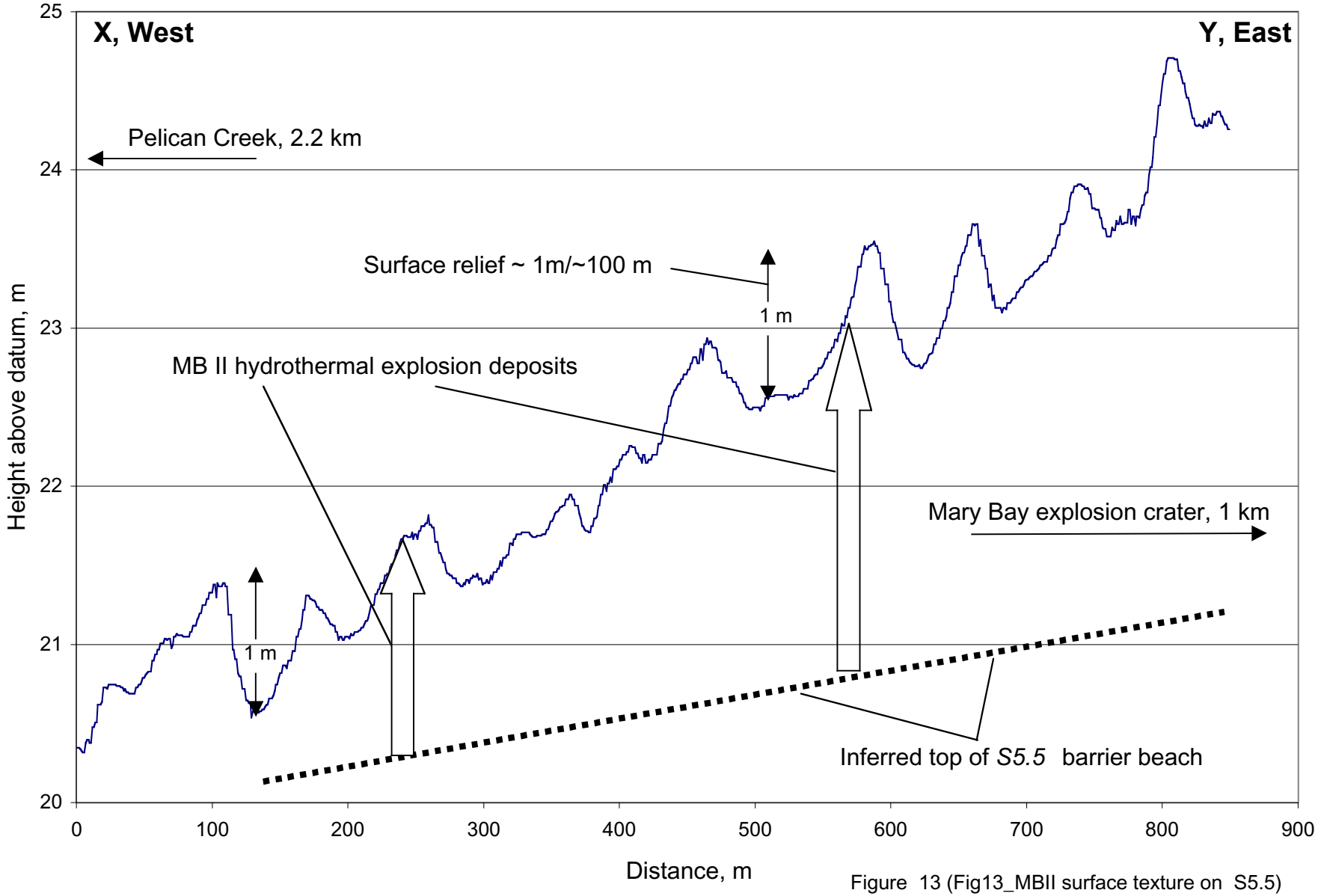

Figure 13 (Fig13_MBII surface texture on S5.5)

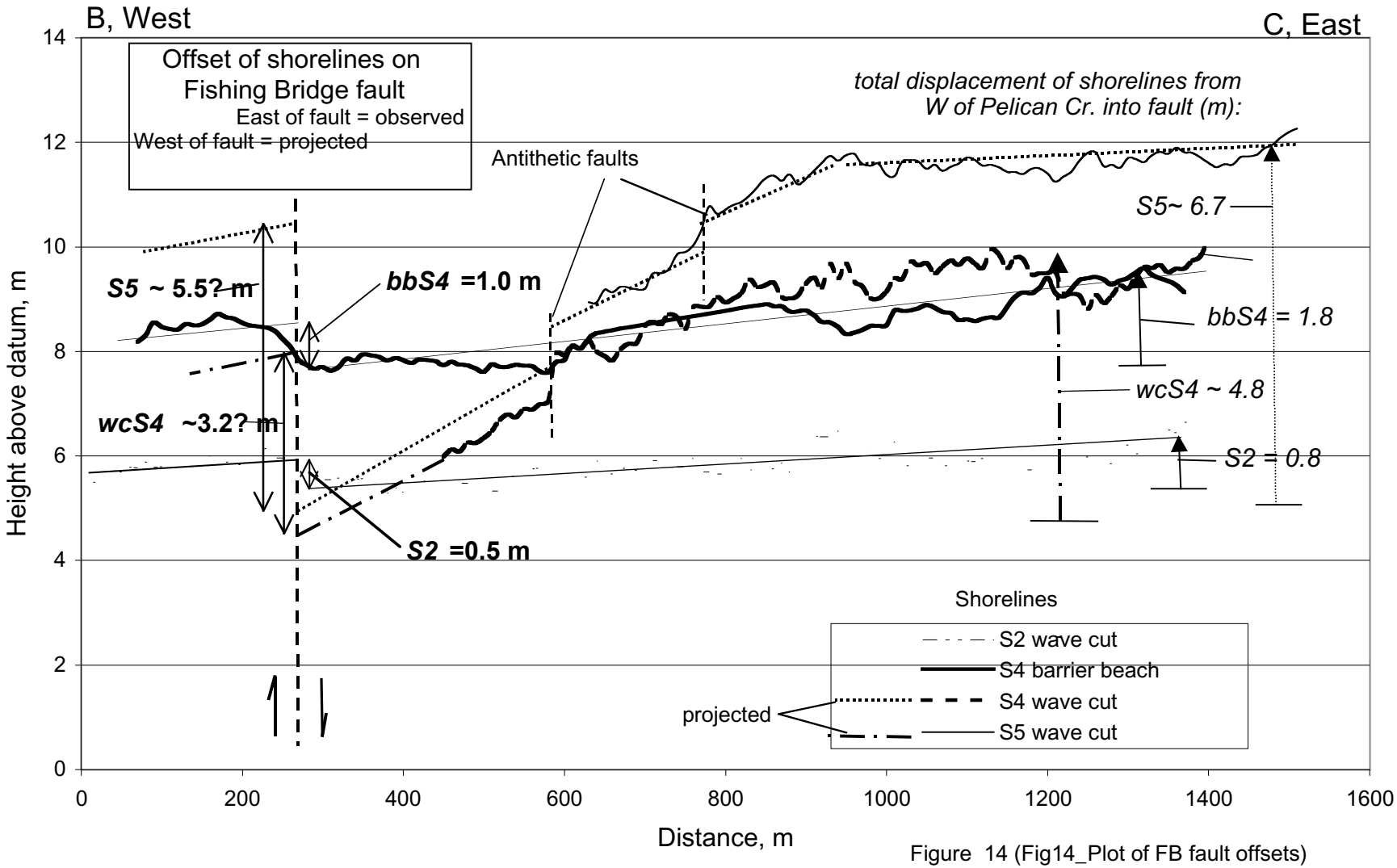

Figure 14 (Fig14_Plot of FB fault offsets)

Figure 15 (Fig15_tilts west from StormPt)

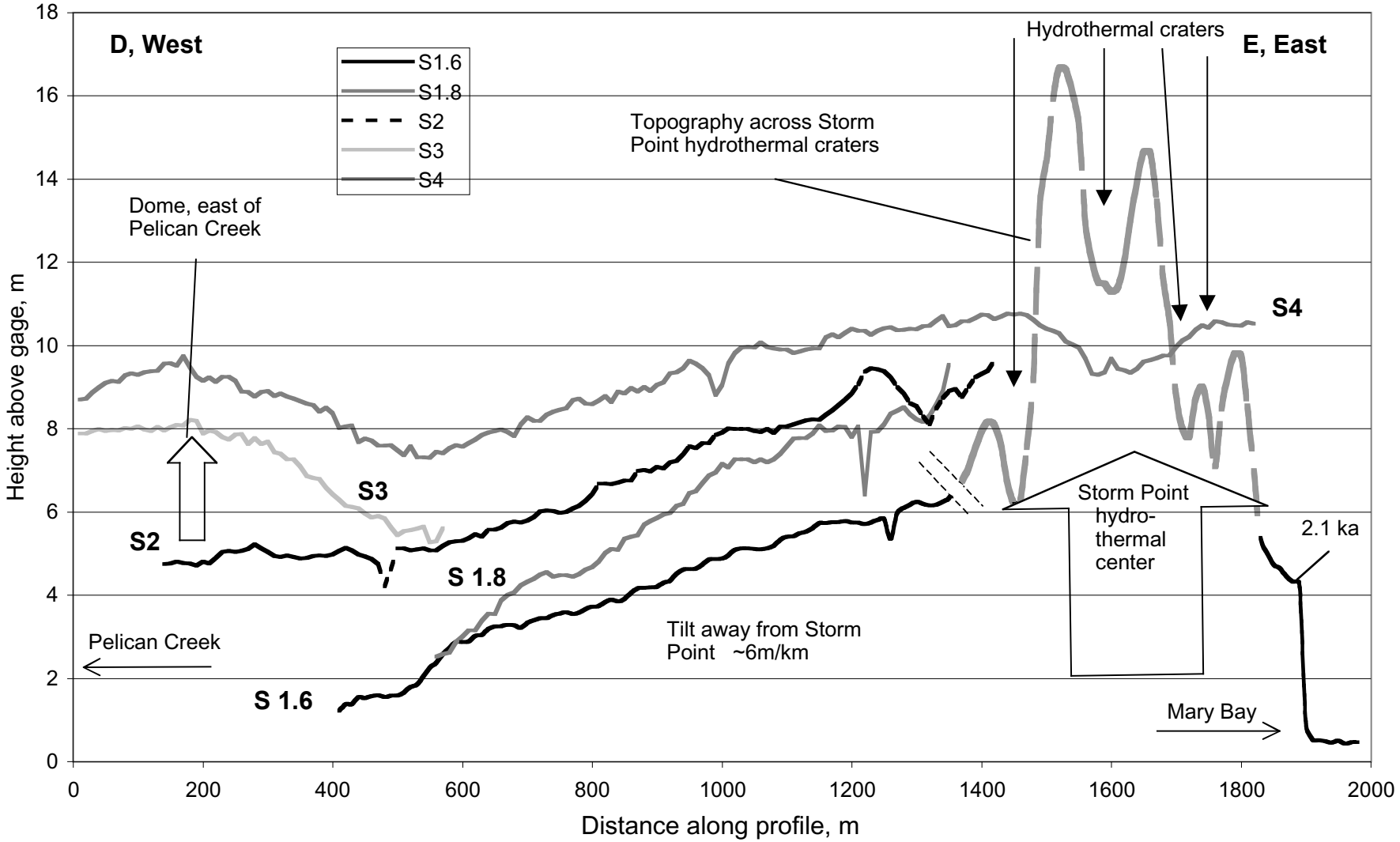

Figure 16 (HB_Fig16.ai)

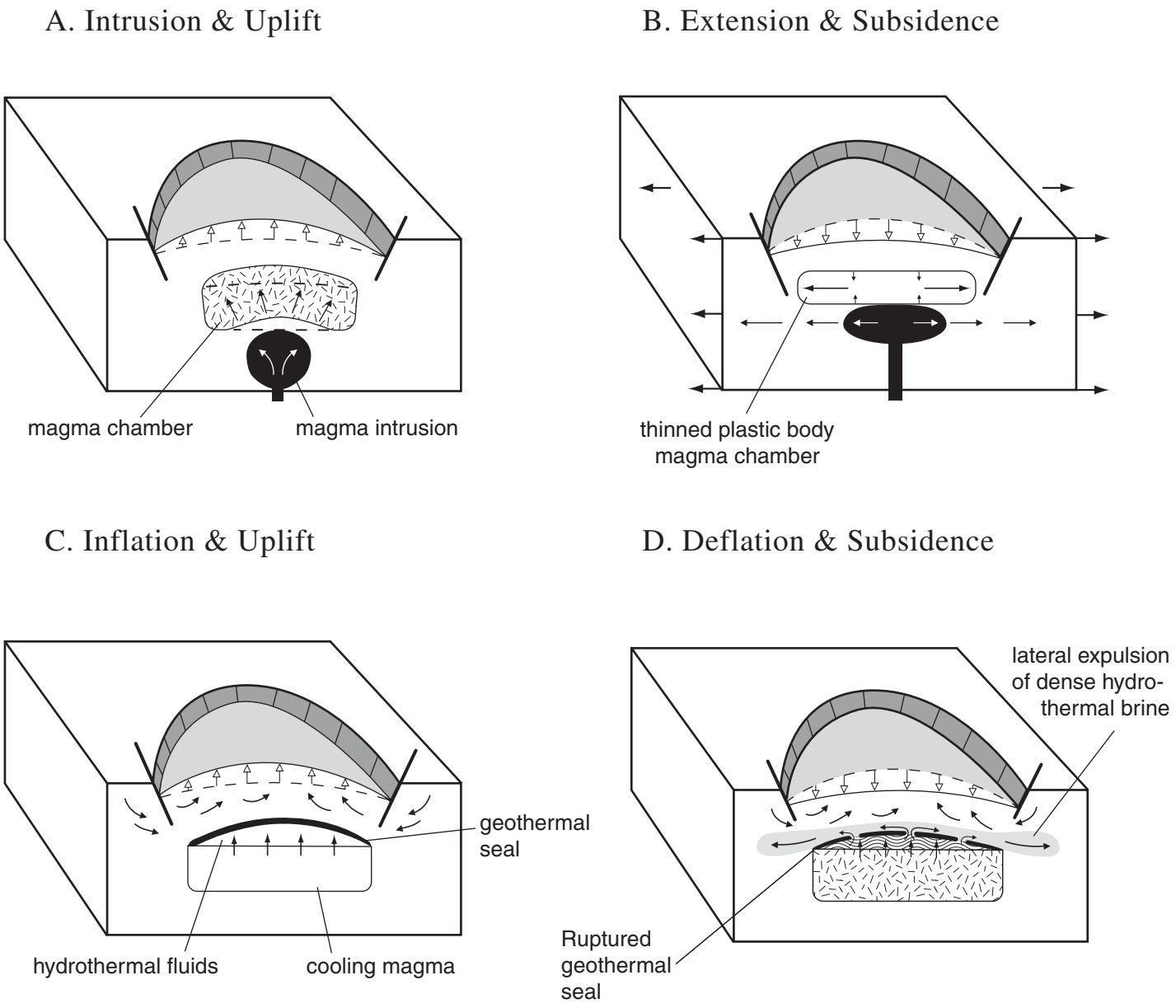

Table 1. Carbon-14 and other ages associated with levels of Yellowstone Lake, generally in order of increasing age. Localities and ages in bold type are critical to interpretation of lake level history

Location & Sample identifier Number in Fig. 4.	Age, yr BP Lab number (s)	Corrected Age & (2 sigma range) Method A	Meters above datum	Remarks
A. Subaerial samples lower than and younger than S-2 shoreline				
1. *Pelican Cr. Paleo-barrier beach* 94p33b, 165 cm	**2,550 ± 60** Beta-78912 CAMS-17814	2,735 (2,362—2,775)	0-1	From depth of 1.65 m in eolian sand, 0.25 m above top of openwork beach gravel near present Yellowstone Lake level.
Pelican Cr. East re-entrant 97P29, 81 cm	2,800 ± 50 WW-1635	2,874_2,917 (2,778—3,057)	4.5m	Charcoal from mixed zone on 4.5 m beach, provides **minimum age** for post-S2 beach.
97P30, 65 cm	2,670 ± 50 WW-1636	2,770 (2,739—2,865)	4 .2	Charcoal from mixed zone on 4.2 m beach, provides **minimum age** for post-S2 beach.
97P31. 65 cm	Modern		?	Pine needles, brown
Storm Point **95P61-90** **95P6-190 cm**	2,160 ± 60 WW-724 CAMS-28372	2,133_2,148 (1, 954—2,335)	3.43	Charcoal from open platy platform gravels related to 4.3 m above datum shoreline on east side of Storm Point. Anomalously young age may be explained by uplift of Storm Point geothermal center.
95P61, 67 (95P6-167 cm	1,160 ± 40 WW-723 CAMS-28371	1,060 (968—1,174)	3.62	Charcoal from eolian deposits overlying the above sample. *May be local uplift of Storm Point*
B. Samples from below present lake level				
2. Drowned YR channel 91P46, 280 cm	2,518 ± 100 _____	2,712_2,622 (2,345—2,837)	-2.37	Wood from 280 cm below slough surface near base of parting sand.
3. Drowned YR channel 92P28, 384 cm	2,560 ± 70 Beta-63807 CAMS-7692	2,738 (2,361—2,781)	-3.08	Pine needles from 353 cm. Depth based on 1991 water levels. Occurs 20 cm above channel gravel
4. Drowned YR channel 91P46, 415-418 cm	**2,750 ± 86** _____	2,848 (2,743—3,136)	-3.39	Charcoal (hard chunk) in gravel at depth of 415-418, 3.85 below water level of slough

5. Drowned YR channel 91P46, 415-423	**2,710±60** Beta-63806 CAMS-7691	2,781 (2,745—2,948)	-3.40	Wood from upper part of gravel at depth of 415-423 cm in drowned paleochannel of Yellowstone River about 1 km downstream from Fishing Bridge
6. West Thumb area 93P3	**2,880 ± 60** Beta-63809 CAMS-7693	2,980 (2,851-3,210)	-4.3	Wood from about 17 feet below lake level of culvert across "north" Little Thumb Creek, West Thumb. Insects indicate wetland environment. Depth 23.5-24 ft below road, est. Altitude 7717 ft. Wood probably conifer but not pine.
7. Bridge Bay, 94P31b, 497 cm	**3,560 ± 60** Beta-78911 CAMS-17813	3,835 (3,690—4,036)	-3.43 approx.	Wood from 497 cm. Upper part of beach sands 40 cm thick in 2.6 m water on 1.8 m soft lake sediments and above firm lake sediments
Pelican Creek drowned valley PC5, 26-27.5 ft	11,720 ± 60 _____	13,805 (13,446—15,123)	-4.3 ?	Carbonized plant fragments or roots. From highway boring at Pelican Creek at depth of 26-27.5 feet, and about 16 feet below present lake level. Sample in lower part of fill near edge of drowned valley of Pelican Creek.
C. Samples lower and younger than S2 and mostly older than submerged shoreline samples.				
Lodge Point sand 97P46A, +85 cm	130 ± 50 WW-1640	2,261 (0—291),	3.7	Charcoal, probably intrusive from above.
97P46F, +65 cm	**2,980 ± 50** WW-1638	3,083_3,205 (2,968—3,335)	3.4	Charcoal near top of fine-bedded sand. Pulse of well-bedded sand into paleo-lagoon with Lodge point soil on S2 shoreline. One possibility is seiche of Yellowstone Lake into basin.
97P46, 45 cm	2,870 ± 40 WW-1845	2,962 (2,868—3,158)	3.2	Charcoal in middle of fine-bedded sand section. Fine-bedded sand deposited rapidly, perhaps during a seiche of Yellowstone Lake .
10. 97P46, 10 cm	**5,300 ± 40** WW-1846	5,998_6,167 (5,937--6,196)	2.85	Charcoal near base of fine-bedded sand. Overlies soil dated 4,110 ± 60 yr BP nearby. Age may be near 3,000 yr based on continuous well-bedded sand section that includes above two samples at 45 and 65 cm.
8. *Lodge Point soil that post-dates S2*. 95P7, 185 cm	**4,160 ± 60** WW-564 CAMS-23265	4,650_4,810 (4,451—4,845)	2.91	Charcoal 20 cm below top of buried soil that formed after lake dropped from S2 level. Soil developed and then was buried by Lodge Point sand (see above) and by eolian deposits. Age of S2 (here at 5.16 m above datum) is significantly greater than these three soil ages.
9. Same as above 95P7, 198 cm	**4,710 ± 60** WW-521 CAMS-22090	5,333_5,466 (5,310—5,591)	2.96	Charcoal sample from 33 cm below top of soil post-dating S2 shoreline and developed and then buried after lake at lower level. Minimum age for S2. Age of S2 significantly greater than these soil ages. .
95P9, 190-200 cm	4,110 ± 60 WW-565 CAMS-23266	4,572_4,778 (4,423—4,831)	~2.8	Charcoal from 20-30 cm below top of buried soil that post-dates S2 shoreline. Age of S2 significantly greater than these soil ages.
D. Samples associated with S-2 shoreline				

11. Terrace cutting S2 95P15, 105-110 cm	**6,740 ± 90** Beta-65468 CAMS-8671	7,587_7,606 (7,432—7,745)	~2.5m Pel. Cr. terrace	From 105-110 cm depth in paleochannel on Pelican Creek terrace that truncates S2 west of Pelican Creek. Top of terrace 1.2 m below S2 at. UTM 550420 East, 493900 North
12. Shoreline below S2 (S 1.6) 97P32B, 70 cm	**6,820 ± 50** WW-1639	7,666 (7,574—7,746)	3.1	Charcoal from base of mixed zone, closely limiting? age for 3-m beach. Also provides minimum age for S2 beach.
13. Archeological excavation on S2, S568/E432	**6,800 ± 90** Beta-65467 CAMS-8670	7,621_7,660 (7,493—7,791)	3.9 S2=4.3 m	At depth of 2.6 m beneath 4.3 S2 surface at east part of Fishing Bridge Peninsula near Pelican Creek terrace (Cannon and others, 1994).
14. S2 on Lodge "bay" 95P4, 94 cm	**7,210 ± 50** WW-563 CAMS-23264	7,979_8,008 7,878—8,158	4.07	Charcoal sample dates time of occupation of S-2 shoreline at 5.16 m AG on Lodge Point. Occurs beneath thick molic soil at depth of 94 cm.
15. S2 on Lodge "bay" 96P50, 53 cm	**7,210 ± 60** WW-1174	7,979_8,008 (7,875—8,168)	4.48	Charcoal in diatomaceous cap of progradational bar deposits of S2 shoreline and provides age for abandonment of S2 shoreline.
E. Possibly associated with S3 shoreline				
16. S3? behind FB Hamilton Store N248-9/W126, level 10	**7,565 ± 70 Beta 63092 ETH 10616**	8,378 (8,190—8,451)	4.75	In old ball field behind Hamilton Store. Site in Fishing Bridge S4 paleolagoon. Sample from level 10 at base of mixed zone Cannon and others, 1994). S3 water may have filled into this area from Yellowstone River.
F. Abandoned S-meander.				
17. Bottom of S-meander 91P34	**7,968 ± 118**	8,781_8,978 (8,457—9,245)	ca 2	Charcoal at auger depth of 109 cm in S-meander.
18. Bottom of S-meander Yell 92-15	**8,030 ± 240** 56712	9,000 (8,371—9,527)	2	Charcoal 2.12-2.20 m BD @ 4.2 m. On top of channel gravel. See below.
19. Bottom of S-meander Yell 92-14, 92P30	**8,250 ± 130** Beta-56711	9,152_9,263 (8,812—9,528)	2.2	Charcoal 2 m below surface and 10-20 cm above river gravel. Dates drowning by rising Yellowstone ponded reach of Yellowstone River. Minimum age for top of Yellowstone River channel gravels that extend down to <1 m AG, and probably <0 m AG. Shorelines S3? and S2 are younger than sample.
G. Samples related to the S4 shoreline				
20. Fishing Bridge Peninsula	**8940 ± 60** Beta-65466	10,154 (9,795—10,219)	7.8 S4 @ 8.2	Charcoal at depth of 1.6 m above beach gravels and in lower part of mixed zone of eolian sand and beach sand. Archeological square near

S375/E512	CAMS-8669			easternmost extent of S4 surface at 9m AG. From northern end on old campground loop. Unit S375/E512 (Cannon and others, 1994, Fig. 44).
21. S4 in Fishing Bridge area	**~8,800 to ~9,400**	9,790-9,890 10,580-10670	9-7.5	Cody complex points (late Paleoindian) on S4 at between Yellowstone River and Pelican Creek (Cannon and others, 1995).
H. Samples associated with hydrothermal explosion deposits				
Indian Pond 96P45, 102 cm	**3,090 ± 50** WW-1173	3,272_3,337 (3,082—3,445))		Charcoal in soil beneath Indian Pond Explosion deposit exposed in culvert excavation for highway half way from Indian Pond east to lake margin. Maximum age for Indian Pond deposit. On S5 shoreline of Meyer and Locke (1986).
Beneath Indian Pond expl. deposit 98P25	4,220 ± 40 WW-2161	4,828 (4,624—4,852)	> S5 shoreline	Charcoal in soil beneath 2.5 m of Indian Pond explosion deposit 0.3 km east of Indian Pond. Actual age near 3 ka, so this was an older charcoal fragment in the buried soil.
Beneath Indian Pond expl. deposit	3,470 ± 130 Beta 48135	3,700_3,716 (3.407—4,089)		Charcoal in soil beneath Indian Pond explosion deposit. On S5
"Little" Storm Point Beneath Indian Pond expl. deposit 95P64B, 32 cm	**3,080 ± 50** WW-725 CAMS-28373	3,270_3,330 (3,082—3,386)	9.4	Humic wetland deposit buried by greenish Indian Pond hydrothermal explosion deposit. Sample 40 cm above shoreline platform at 8.95 m above datum.
Beneath Indian Pond expl. deposit	3,500 ± 250 W-2734	3,727_3,825 (3,170—4,501)		Sample beneath diamicton now recognized as Indian Pond hydrothermal explosion deposit. Richmond, 1976, section 74. Occurs above Mary Bay II explosion deposit.
"Little Storm Point" section 96P47. + 140 cm	430 ± 50 WW-1169	505 (323—539)		Charcoal in weak soil in eolian sand 40 cm below surface.
96P47 + 47 cm	420 ± 50 WW-1166	502 (319—536)		Charcoal in soil in eolian sand 160 cm down.
96P47, 0 cm	1,780 ± 40 WW-1164	1,707 (1,570—1,820)		Charcoal. Overlies Indian Pond deposit and provides minimum age for it and for base of eolian sand.
96P47, -40 cm	**2,940 ± 60** WW-1165	3,078_3,154 (2,890—3,323)	8.95	Charcoal. Immediately underlies Indian Pond explosion deposit and provides best maximum age for deposit.
96P47, -70-75 cm	5,160 ± 60 WW-1167	5,916 (5,748—6,167)		Charcoal in soil pendant on platform of S4.5? shoreline cut across Mary Bay II explosion deposit.
96P47, -75 cm	3,970 ± 50 WW-1168	4,419 (4,259—4,566)		Blackened material including charcoal. Similar to above.
95P53 103 cm	4,040 ± (60) WW-722	4,451_4,521 (4,412—4,806)	8.06	Sample below 2 buried soils in tree throw wedge pulled from platform gravels of 7 m S4? Shoreline.

	CAMS-28370			
95P10B- 85 cm	4,050 ± 60 WW-522 CAMS-22091	4,453_4,524 4,411—4,813		Charcoal below buried soil in disturbed zone 20cm above platform gravels at ~7 m above datum in bluffs south of Indian Pond.
95P64B 48-50 cm	5,290 ± 60 WW-726 CAMS-28374	5,922_6,166 (5,922—6,271)	9.2	Charcoal fragments in molic buried soil above stone line of platform of 10.6m S5 (?) shoreline that is eroded on Mary Bay II explosion deposit.
98P11	5,890 ± 40 WW-2157	6,678_6,722 (6,574—6,844)	8.36	Charcoal at base of platform gravels very close to the S4? shoreline. Overlain by buried soil and by Indian Pond explosion deposit. From east of 8 ka samples.
Indian Pond Creek West section 95P6c, 80 cm	2,200 ± 50 WW-720 CAMS-28368	2,156_2,298 (2,060—2,340)	13	Charcoal in eolian sand deposit above level of sample 95P51. May be intrusive from above.
Indian Pond Creek West 95P51, 105 cm	8,160 ± 50 WW-721 CAMs-28369	9,032_9,124 (9,007—9,394)	10	Charcoal in sheet-bedded sands about 10 cm above platform gravel of pre-S4 lake level ~11 m above datum when Mary Bay II explosion deposit pre-dates S4? shoreline and post-dates Glacier Peak ash (11,400 yr BP) and age of 11,400 yr BP Scott Elias obtained on insect in fibrous lacustrine peat deposit.
Indian Pond Creek West	11,400 ± 90 CAMS-17388	13,411 (13,042—13,800)	~4.8?	Caterpillar mandibles from lacustrine stringy peat about 1 m above Glacier Peak ash and several meters below Mary Bay II explosion deposit.
Lake bluffs by Indian Pond 95P66	**8,110** ± 60 WW-727 CAMS-28375	9,025 (8,791—9,262)	7.64	Charcoal from grass and brush fire above platform gravels at 7.64 m above datum S4? shoreline at ~9 m above datum. Occurs below two phases of Indian Pond deposit.
98P14	**8,340 ± 40** WW-2159	9,328_9,419 (9,150—9,484)	7.0	Charcoal from platform gravel (base 6.9 m top 7.15) of nearby S4? shoreline that truncates Mary Bay II hydrothermal explosion deposit. Overlies lake sediments on Mary Bay II hydrothermal explosion deposit.
98P13	**8,210 ± 40** WW-2158	9,132_9,243 (9,027—9,397)	7.0	Charcoal from platform gravel of S4? Site at same position and very near 98P14. Overlies lake sediments on Mary Bay II hydrothermal explosion deposit.
Richmond, 1977, section 74	10,720 ± 350 W-2738	12,857 (11,344—13,437)	~5-6?	Charcoal 2.6 m above Glacier Peak ash and beneath Mary Bay II explosion deposit.
Glacier Peak ash	11,450 ± 50yr BP	13,436 (13,160-13,800)	~2.8	Below MB II explosion deposit and beneath "S4?" and by inference S5 shoreline. Collected by Ken Pierce and determined by A. Sarna to have mixture of shards of both Glacier Peak and Yellowstone affinities. Probably same ash 2.92 m above datum at Richmond's section (1976,
	12,100 ± 50 yr BP	14,100 (13,690-15,360)		

	11,200 ± 50? yr BP	13,155 (12,910-13,750)		Section 74). First two ages from Whitlock (1993), third from Mehringer and others (1984), and last from Doerner and Carrara, (2001).
	>11,510 ± 70 yr BP	13,460 (13,170-13,820)		
Turbid Lake explosion deposit 98P21B	8,410 ± 40 WW-2160	9,437_9,469 (9,300—9,525)	~76 m	Charcoal from high in bluff of Bear Creek beneath 2 meters of Turbid Lake explosion deposit. Altitude near 7,800 ft.
"	8,000 ± 500 W-2486	8,819_8,986 (7,792—10,190)	"	Sample of charcoal from beneath Turbid Lake explosion deposit along Bear Creek. Section 58 of Richmond, 1977. Air conditioning problem in lab at time of analysis.
"	8,310 ± 300 W-1944	9,300_9,398 (8,435--10,150)	"	Sample collected by Dave Love from beneath diamicton now considered to be Turbid Lake explosion deposit.
I. Old lake sediment ages				
Bridge Bay Marina 94P23, 897 cm	11,890 ± 60 Beta 78910 Cams 17812	13,840 (13,624—15,250)	-7.97	Twigs from 8.97 below platform (0.27 m above water surface on 8/5/94) with beach? sand at about 4 m below datum.
Lodge Point Yell 92-13	13,040 ± 90 Beta-56710	15,678 (14,605—16,173)	~3?	Sedge peat 30-40 cm below Theriott's diatomite. Old carbon dioxide effect?
Lodge bay	13,360 ± 320 Beta 40764	16,053 (14,622—16,928)	~3?	Sedge peat, Lodge Point, collected by Wayne Hamilton.
J. Samples from Southern part of Yellowstone Lake				
22. 00P52 & archeological site 48YE409	**9,360 ± 60** Beta 148567	10,570 (10,294-10,737)	5.8	Charcoal from base of mixed zone on shoreline gravels that are the 7.0 m S4 of Locke (written commun., 2000). Site 1 km east of Grant Village sewage disposal plant.
23. 48YE409 *2000-. Osprey Beach site*	**~8,800 to 9,400**	9,790-9,890 to 9,603-11,035	~5.8	Same as 00P52. Point types of late Paleoindian age in the 8,800-9,400 yr BP time range. Cody points in base of mixed zone above beach gravels to 5.7 m above datum on 7.4 m S4 of Locke, written commun., 2000. May contain older point.
Plainview point from near above samples.	~500 years older than Cody Complex	~10 to 11.6 ka (see above)	?~5.8	A Plainview point was found either (1) recently slumped to the present beach (Ann Johnson, personnel commun., 2002) or (2) inland 30 m and on a surficial linear concentration of archeological material (Don Blakeslee, personnel commun., 2002).
Eagle Bay	4,540 ± 40 ETH 3987	5,294 (5,046—5,317)		Colluvium on fault scarp eroded by S4 shoreline (Locke and others, 1992)

Samples associated with S2 97P54, 215 cm	**6990 ± 40** WW-1848	7,790_7,815 (7,689—7,933)	5.5	Wood near base of paleochannel in Yellowstone delta agraded to ~9 m above datum or ~7,760-65 ft alt. This landform dams off Trail Lake (7,751 ft, see below). Age approximate age of S2 shoreline in NW part of lake
Yellowstone River Delta	**7,215 ± 70** _____	7,980_8,010 (7,871—8,17)	Lake 6.1	Basal age from Trail Lake, inferred to be deposited behind the S2 delta of the Yellowstone River. Trail Lake altitude 7,751 ft.
Sites in or near modern Yellowstone River delta				
97P51, 51 cm depth	1,570 ± 40. WW-1847	1420_1508 (1,350—1,541)	~2m	Dead duck delta 5 feet above present lake. In kettle lake connected to Yellowstone Lake northwest of Trail Creek cabin Delta top about 7,738 ft.
97P56, 56 cm depth	850 ± 40 _____	738 (674—908)	~1 m	Stabilized beach with grass and trees at 7,739 ft, east side of delta.
97P55, 240 cm depth	340 ± 40 WW-1849	328_431 (301—504)	~1 m.	Point of modern delta.

Table 2. Offsets on the Fishing Bridge fault and associated tilting across the Fishing Bridge peninsula (Fig. 5) based on offset shorelines and shoreline projections shown in Figure 14.

Shoreline/Age	**Height, m** above datum	**Tilt[1] , m**	**Total Offset, m**	**Offset/tilt**	**Interval offset**
***S2*/8.0 ka**	6	0.8	0.5 m	63%	0.5 m
Bb *S4*/10.7 ka (barrier beach	9	1.8	1.0	55%	0.5 m ?
wc *S4*/10.7 ka (wave cut	9	~4.8	~2.9[2] – 3.2[3] m	(60%)[2]	1.9-2.2 m
***S5*/12.6 ka**	12	≈6.7	≈4.0 [2] - 5.5[3] m	(60%)[2]	1.1-2.3 m

[1] Tilt across Fishing Bridge Peninsula to Fishing Bridge fault.Ä
[2] Offset based on offset tilt ratio of 60% as determined from S2 and bbS4.Ä
[3] Offset based on projection to of wcS4 and S5across fault as shown in Figure 14.Ä

Table 3. Submerged lake and river levels and their normalization to the outlet.

Location	Le Hardy Rapids (LHR)	Drowned channel to Outlet	Bridge Bay	Little Thumb Cr.-N
1923-1975 parameters				
1. 1923-75 uplift	800 mm	600 mm	470 mm	460 mm
2. Δh to LHR (1923-76)	0	200 mm	330 mm	340 mm
3. Δh site /Δh @ Outlet	---	1 x	1.65 x	1.70 x
4. #2 / Δh-LHR, % total	0%	25%	41%	43%
Old submerged sites				
5. A. Age, yr BP		2,750	3,560 ± 60	2,880 ± 60
B. Corrected age, years		2,848	3,835	Est. 2,970
6. Depth *below* datum			3.43 m	4.3 m
7. Depth below S1 (Present Lake) (1.8 m + #6)			5.2 m	6.1 m
8. #7 / #3 (normalized to outlet)			3.2 m	3.6 m
*9. Total ΔH to LHR = #7 + 5m**		*(8.5 m)*	*10.2*	*11.1m*
10. Normalized to outlet, Δh to LHR, #8 + 5m[1]		**(8.5 m[2])**	**8.2 m**	**8.6 m**
11. Net rate to present between site and LHR, (#10/#5B)		3.0 mm/yr	2.7 mm/yr	3.9 mm/yr
12. Rate (1923-75), site to LHR (#2/52 yrs)		3.9 mm/yr	6.3 mm/yr	6.5 mm/yr

5m[1] = paleoriver gradient, outlet to Le Hardy Rapids (LHR) at 1m/km.

(8.5 m[2]) = total for reach of Yellowstone River from outlet to LHR based on total river gradient of 5 m and 3 m vertical distance of paleo-channel gravel below bedrock threshold at LHR (Fig. 6).

Table 4. Processes for decreases, increases, and oscillations in Yellowstone Lake and River level in post-glacial time. See text under headings and letters for more complete discussion. Processes in this type discussed further in text: processes in this type discussed only in this table. The observed historic changes and the present drowned "outlet reach" of the Yellowstone River suggest changes in the level of Le Hardys Rapids are important.

CHANGE & PROCESS	COMMENTS
I. Decrease in lake level	
A. Glacial damming	A. During glacial recession, glaciers from Beartooth uplift dammed lakes in Yellowstone Lake-Hayden valley area, particularly above S6 level.
B. Outlet erosion	B. At Le Hardys Rapids, very resistant threshold formed by 1-3 m ledge with interlocking micro-spherulites near base Lava Creek Tuff. Much more erodible units above and below.
C. Magmatic cooling	C. Contraction due to cooling of batholith beneath Yellowstone caldera. Subsidence estimated to be 0.6-0.7 mm/y by Fournier and Pitt (1985).
D. Tectonic stretching	D. Crustal thinning and downwarping above magma chamber and other ductile material.
E. Yellowstone Lake ceasing to overflow	E. A greater than likely drying of climate, for loss from lake now about 15% by evaporation and 85 % by overflow.
II. Increase in lake level	
A. Magma intrusion and inflation	A. Magma and associated heat are probably being added from hotspot source. Magma likely to be permanent volumetric addition to caldera unless intruded radially to outside caldera.
B. Tectonic compression	B. Local compression particularly squeezing a ductile magma chamber could produce doming.
III. Possible increases or decreases in lake level	
A. Faulting	A. Faulting of appropriate magnitude and timing not apparent. Overall sag of shorelines and offset on Fishing Bridge fault noted in outlet area.
B. Glacial-isostatic rebound	B. Glacial load nearly uniform over Yellowstone Lake basin, which would produce smooth uplift. Rebound mostly during deglaciation because brittle-ductile transition shallow.
IV. Oscillations in lake level	
A. Geothermal inflation and deflation	A. Geothermal sealing, pressure buildup, and inflation followed by rupture of seal, release of geothermal fluids, and deflation. A cycle produces no net change in level consistent with paleoshorelines not rising towards caldera center.
B. Combinations from increase and decrease	B. For *increase*, A magna intrusion, is most plausible, for *Decrease* D tectonic stretching is favored, although A and B may also be occurring.

Table 5. Change in elevation of *S2*, *S4*, and *S5* from near the caldera axis in the outlet, to sites farther away but in the caldera, to sites outside the caldera. The first number followed by "m" is the shoreline elevation above datum. The number in kilometers (km) is the distance from the caldera axis of historic uplift (see Fig. 1). For the outlet area, elevations are for the eastern part of the Fishing Bridge peninsula.

Shoreline and age	Site in outlet area	Site in caldera but farther from axis.	Site outside caldera	Vertical decrease in height towards caldera axis over distance.
S2 8.0 ka	5m/4 km 8.0	------	7-8 m/35 km Delta in SE arm 8.0 ka	2-3 m/30 km
S4 10.7 ka	8-9 m/4 km	7 m/17 km S shore, West Thumb	-------	-1 to -2 m/13km, *increase* towards caldera axis
*S5** 12.6 ka	10-13m/4 km	14 m/13 km Caldera margin at Lake Butte	19 m/35 km* Yellowstone River delta area	6-9 m/31 km total. 5 m/22 km outside caldera, 1-4 m/9 km. inside caldera.

**S5* uses elevation as shown in Figure 10 to Mary Bay crater wall, where *S5* is the same as *S7* of Locke and Meyer (1994, Figure 4) and thus continues the same as S7 of Locke and Meyer (1994) along the east shore of Yellowstone Lake.